



저작자표시-비영리-변경금지 2.0 대한민국

이용자는 아래의 조건을 따르는 경우에 한하여 자유롭게

- 이 저작물을 복제, 배포, 전송, 전시, 공연 및 방송할 수 있습니다.

다음과 같은 조건을 따라야 합니다:



저작자표시. 귀하는 원저작자를 표시하여야 합니다.



비영리. 귀하는 이 저작물을 영리 목적으로 이용할 수 없습니다.



변경금지. 귀하는 이 저작물을 개작, 변형 또는 가공할 수 없습니다.

- 귀하는, 이 저작물의 재이용이나 배포의 경우, 이 저작물에 적용된 이용허락조건을 명확하게 나타내어야 합니다.
- 저작권자로부터 별도의 허가를 받으면 이러한 조건들은 적용되지 않습니다.

저작권법에 따른 이용자의 권리는 위의 내용에 의하여 영향을 받지 않습니다.

이것은 [이용허락규약\(Legal Code\)](#)을 이해하기 쉽게 요약한 것입니다.

[Disclaimer](#)

Master's Thesis

Prediction of cutting forces and delamination
during carbon fiber reinforced plastics (CFRP)
machining

Yeong-Bin Kim

Mechanical Engineering
Graduate School of UNIST

2017

Prediction of cutting forces and delamination
during carbon fiber reinforced plastics (CFRP)
machining

Yeong-Bin Kim

Mechanical Engineering
Graduate School of UNIST

Prediction of cutting forces and delamination during carbon fiber reinforced plastics (CFRP) machining

A thesis/dissertation
submitted to the Graduate School of UNIST
in partial fulfillment of the
requirements for the degree of
Master of Science

Yeong-Bin Kim

06. 13. 2017
Approved by

Advisor
Hyung-Wook Park

Prediction of cutting forces and delamination
during carbon fiber reinforced plastics (CFRP)
machining

Yeong-Bin Kim

This certifies that the thesis of Yeong-Bin Kim is approved

06. 13. 2017

Hyung Wook Park

Young Bin Park

Nam Hun Kim

Abstract

Carbon Fiber Reinforced Plastic (CFRP) has been widely used in various industrial areas due to its corrosion resistance, stiffness and high strength-to-weight ratio. However, the machining process of CFRP composite material is complex compared to that of metals. The reason is the unique properties of CFRP composite, such as anisotropy and inhomogeneous characteristics. Therefore, many defects, such as uncut fiber, delamination and tool wear, occur in the process of CFRP machining. To prevent defects in CFRP machining, we discuss important factors, cutting mechanism and chip formation. Based on these, numerical models are suggested for cutting forces and damage prediction. It will help optimize machinability and productivity of CFRP machining.

In this study, we developed numerical solutions to predict cutting forces along the fiber orientation in each machining condition in CFRP orthogonal cutting. There are preliminary force prediction model and force prediction model according to varying fiber orientation. The first one is from Bhatnagar's CFRP force prediction model. This model is proved with CFRP orthogonal cutting in each fiber orientation. This model shows that cutting force and thrust force are increased as increasing feed rate similar to the experimental results. High feed rate can increase the depth of cut in machining. This developed model is more accurate than Bhatnagar's model in wider area in the condition of high feed rate. The reason is that epoxy region contained in preliminary force prediction model rises in wider area.

The other model is modified force prediction model for varying fiber orientation. This model was expanded from Zhang's CFRP force model. Zhang commented this cutting mechanism can be applied only in fiber orientation below 90° . He proved this in low speed CFRP cutting experiments. We did CFRP orthogonal cutting in high cutting speed over 80m/min. We applied similar cutting mechanism into modified model along all the fiber orientation from 0° to 180° . Force prediction model for all the fiber orientations has similar tendency as the experimental results. The prediction credibility is from 50% to 98.5%. Errors can be generated by many factors in CFRP machining.

From this modified force prediction model for varying fiber orientation, damage prediction model can be suggested referring to Jahromi's damage prediction model. It is based on energy balance in each fiber material. This damage prediction model has similar curve tendency as experimental results. It shows no defect along the fiber orientation from 0° to 90° . However, in the range of fiber orientation from 90° to 180° , it starts making defects inside UD CFRP workpiece because of fiber crush. It is verified by CT X-ray internal inspection. We need to consider poor machinability in the range of fiber orientation over 90° . In conclusion, this process will help optimize machinability in CFRP machining.

Contents

I . Introduction -----	1
1.1 Background -----	1
1.2 Research objectives and approach -----	2
1.3 Dissertation organization -----	4
II. Literature review -----	6
2.1 Mechanism of Carbon Fiber Reinforced Plastics machining -----	6
2.2 Characteristics of Carbon Fiber Reinforced Plastics machining -----	8
2.2.1 Cutting forces in CFRP orthogonal machining -----	9
2.2.2 Fiber orientation in CFRP orthogonal machining -----	9
2.2.3 Chip formation in CFRP orthogonal machining -----	10
2.2.4 Delamination in CFRP orthogonal machining -----	11
2.3 Numerical solutions to predict force in CFRP machining -----	11
2.4 Flow of research about theoretical solution to predict force and delamination in CFRP machining -----	12
III. Numerical modeling -----	19
3.1 Numerical model for predicting force -----	19
3.1.1 Preliminary model for predicting force -----	19
3.1.2 Numerical model for predicting force according to varying fiber orientation -----	21
3.1.2.1 Region 1 - Chipping -----	22
3.1.2.2 Region 2 - Pressing -----	23
3.1.2.3 Region 3 - Bouncing -----	25
3.1.2.4 The total cutting forces -----	26
3.2 Numerical model for predicting damage -----	27
IV. Experimental validation -----	30
4.1 Experimental validation of preliminary model for predicting force -----	30
4.1.1 MD CFRP property test -----	30
4.1.1.1 Tensile test -----	30
4.1.1.2 Friction test -----	32
4.1.2 Experimental setup -----	33
4.1.3 Comparison between experimental and analytical results -----	35
4.1.4 Summary -----	37

4.2 Experimental validation of numerical model for predicting force and damage according to varying fiber orientation -----	37
4.2.1 Experimental set -----	37
4.2.2 Comparison between experimental and analytical results -----	38
4.2.3 Summary -----	43
4.3 Experimental validation of modified model for predicting damage -----	43
4.3.1 Experimental setup -----	44
4.3.2 Comparison between experimental and analytical results -----	44
4.3.3 Summary -----	46
V. Conclusions -----	48
5.1 Summary -----	48
5.2 Conclusions and contributions -----	49
5.3 Future work -----	50
VI. Acknowledgement -----	51
VII. References -----	52

List of figures

Figure 1-1. Global demand for carbon fiber from 2008 to 2020 -----	1
Figure 1-2. (a) Uni-direction(UD) CFRP, Multi-direction(MD) CFRP, (b) Fabric CFRP -----	2
Figure 1-3. Parameters and types of numerical modeling -----	3
Figure 1-4. Flow chart for the organization of the dissertation -----	5
Figure 2-1. The XXsys carbon fiber jacket site filament winding technique (USA) -----	6
Figure 2-2. Schematic of orthogonal cutting; (a) Metals, (b) UD-FRP -----	7
Figure 2-3. Types of milling operations -----	8
Figure 2-4. Machinability of CFRP drilling -----	8
Figure 2-5. Cutting force diagram in CFRP orthogonal cutting -----	9
Figure 2-6. Fiber orientation relative to the cutting direction -----	10
Figure 2-7. Chip morphology SEM photos of carbon fiber with orientation angles along the fiber direction; (a) $0^\circ \leq \theta < 90^\circ$ fiber orientation, (b) $90^\circ \leq \theta < 180^\circ$ fiber orientation -----	10
Figure 2-8. Comparison of experimental and analytical results for predicting damage -----	11
Figure 2-9. Cross section of specimens in CFRP cutting; (a) fiber angle 90° , (b) 0° -----	13
Figure 2-10. Cutting mechanisms in the orthogonal machining of composite -----	13
Figure 2-11. Cross section of specimens in CFRP cutting; (a) fiber angle 90° , (b) 180° -----	14
Figure 2-12. Orthogonal cutting model of composite -----	14
Figure 2-13. The cutting diagram in CFRP orthogonal machining; (a) Region 1, (b) Region 2, and (c) Region -----	16
Figure 2-14. Comparison between numerical model predictions and experimental results of MTM56 in (a) thesis, (b) using MATLAB code -----	16
Figure 2-15. Schematic of a single fiber under lateral force -----	17
Figure 2-16. Effect of fiber orientation in surface roughness -----	18
Figure 3-1. Schematic of CFRP orthogonal cutting -----	19
Figure 3-2. Flow chart for force prediction model according to varying fiber orientation -----	21

Figure 3-3. Schematic of CFRP orthogonal cutting -----22

Figure 3-4. Schematic of CFRP orthogonal cutting in Region 1 -----23

Figure 3-5. Schematic of CFRP orthogonal cutting in Region 2 -----24

Figure 3-6. Schematic of CFRP orthogonal cutting in Region 3 -----26

Figure 3-7. Flow chart for showing the organization of damage prediction model -----27

Figure 3-8. Schematic of micro-scale cutting mechanism in CFRP machining -----28

Figure 4-1. Tensile test of MD CFRP by INSTRON 5982 -----30

Figure 4-2. Stress-strain curve of MD CFRP tensile test; (a) 20°, (b) 40°, (c) 60° -----31

Figure 4-3. Tensile strength of each fiber orientation in tensile test -----32

Figure 4-4. Friction coefficient of each fiber orientation in friction test -----33

Figure 4-5. Workpiece of MD CFRP orthogonal cutting -----34

Figure 4-6. Drawings of jig and key for CFRP orthogonal cutting-----34

Figure 4-7. Experimental setup of the orthogonal machining for CFRP material -----35

Figure 4-8. Comparison between numerical and experimental results in terms of (a) cutting forces and (b) thrust forces with cutting speed, 80m/min and feed rate, 0.15mm/rev -----36

Figure 4-9. Comparison between numerical and experimental results in terms of (a) cutting forces and (b) thrust forces with cutting speed, 80m/min and feed rate, 0.21mm/rev -----36

Figure 4-10. Workpiece of UD CFRP orthogonal cutting -----38

Figure 4-11. Cutting forces in UD CFRP orthogonal cutting with cutting speed, (a) 80m/min, (b) 6m/min and feed rate, 0.15mm/rev -----39

Figure 4-12. Microscopic image: chip formation in UD CFRP machining with cutting speed 80m/min in (a) $\theta < 90^\circ$, (b) $90^\circ \leq \theta$ and 6m/min in (c) $\theta < 90^\circ$, (d) $90^\circ \leq \theta$ -----40

Figure 4-13. Comparison between numerical and experimental results in terms of (a) cutting forces and (b) thrust forces with cutting speed, 80m/min and feed rate, 0.05, 0.10, 0.15mm/rev -----40

Figure 4-14. Comparison between numerical and experimental results in terms of (a) cutting forces and (b) thrust forces with cutting speed, 120m/min and feed rate, 0.05, 0.10, 0.15mm/rev -----41

Figure 4-15. Comparison between numerical and experimental results in terms of (a) cutting forces and (b) thrust forces with cutting speed, 160m/min and feed rate, 0.05, 0.10, 0.15mm/rev -----41

Figure 4-16. Microscopic image: tool round-edge by scanning electron microscope(SEM) -----42

Figure 4-17. CT X-ray image: internal delamination of UD CFRP machining with cutting speed,
80m/min and feed rate, (a) 0.05, (b) 0.10, (c) 0.15mm/rev -----45

Figure 4-18. Comparison between numerical and experimental results in terms of damage length
with cutting speed, 80m/min and feed rate, 0.05, 0.10, 0.15mm/rev -----46

List of tables

Table 4-1. Tensile strength and shear strength of each fiber orientation -----	32
Table 4-2. List of overall UD CFRP composite material's properties -----	38
Table 4-3. Cutting forces prediction error with cutting speed, 80m/min -----	41
Table 4-4. Cutting forces prediction error with cutting speed, 120m/min-----	42
Table 4-5. Cutting forces prediction error with cutting speed, 160m/min -----	42
Table 4-6. List of fiber and epoxy material's properties in UD CFRP composite -----	44
Table 4-7. Error percentage of damage length prediction model with cutting speed, 80m/min ----	46

1. Introduction

1.1. Background

Carbon Fiber Reinforced Plastic (CFRP) has extremely good strength and light material which contains carbon fibers and resins. It means that CFRP has high strength-to-weight ratio. This composite material has great dimensional stability and corrosion resistance compared to metal alloys [1-3]. Demands of CFRP is increasing rapidly. These days, CFRP is representatively used as aerospace, automotive, and sports goods. Its application has been increased rapidly and it will consist this tendency as shown in **Fig. 1-1**.

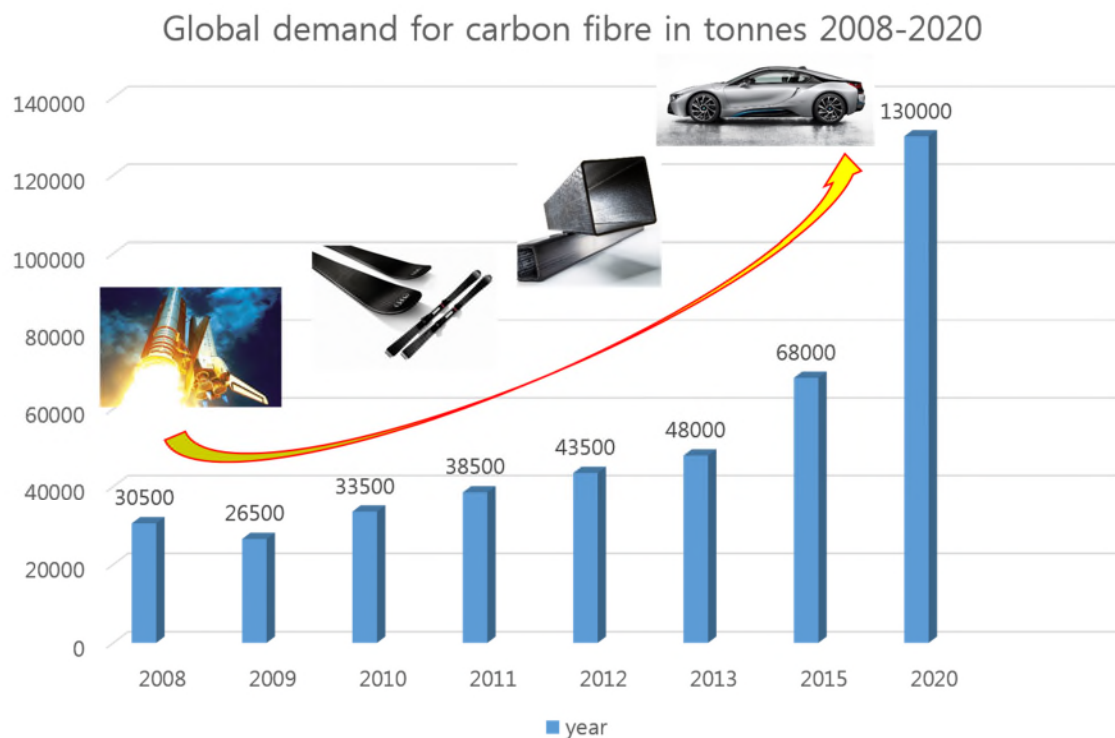


Fig. 1-1 Global demand for carbon fiber from 2008 to 2020

[Mark Holmes et al. (2014), materialstoday]

However, CFRP is somewhat difficult to be applied to the industry because it is anisotropic and inhomogeneous different from metal's physical properties [4, 5]. In CFRP machining, it decreases the attachment between fibers and resins. And it causes delamination to be generated [6].

Delamination is representative of defects in CFRP machining. Since there are many defects, such as delamination and tool wear during machining of CFRP composites, the optimization of machining is essential to improve the productivity. For machinability, it must be prevented. For applying it to the industries, its machinability is the most important point. Many engineers try to improve the machinability in CFRP machining.

There are three kinds of CFRP as Uni-direction (UD) CFRP, Multi-direction (MD) CFRP, and Fabric CFRP depending on methods of manufacturing. As shown in **Fig. 1-2**, UD CFRP is composed of only one same direction in each stack floor. MD CFRP has $0^{\circ}/90^{\circ}$ stack floors. Lastly, fabric CFRP has fibers woven. In this research, UD CFRP and MD CFRP are used.

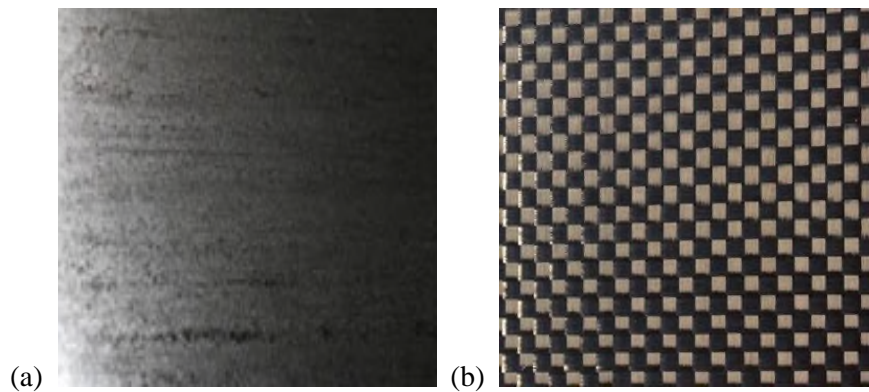


Fig. 1-2 (a) Uni-direction(UD) CFRP, Multi-direction(MD) CFRP, (b) Fabric CFRP

1.2. Research objectives and approach

This research is basically about orthogonal machining of Carbon Fiber Reinforced Plastics (CFRP). This is important for dimensional accuracy and better surface finish in machining. Composite materials' characteristics are introduced previously. CFRP has different characteristic from the metal. Representatively, it is anisotropic and inhomogeneous. Therefore, the machining of CFRP is more complicate than that of metal. Fiber orientation, brittle behavior and other mechanisms are considered. This paper is motivated to develop some models by specific mechanism to predict the cutting forces along the fiber orientation. This study suggest two kinds of force prediction numerical models. The first one is preliminary model applied by Bhatnagar force prediction model [7]. The second one is modified model according to varying fiber orientation applied by Zhang L.C. CFRP machining mechanism and force prediction model [8].

For this prediction validation with experiments, orthogonal machining of CFRP is proper to consider them. It is because CFRP orthogonal cutting is easy to find out characteristics of CFRP along the fiber orientation. This research would be helpful for optimization and productivity in CFRP

machining.

In addition, according to the parameters such as material properties, feed rate, and cutting speed, the force and machinability are affected. These parameters are considered when some numerical models are constructed like **Fig. 1-3**.

The goal of this research is to develop theoretical and numerical prediction models for analyzing the cutting forces in Carbon Fiber Reinforced Plastics (CFRP) machining and to experiment CFRP orthogonal machining for analyzing the characteristics of composite materials. The parameters are presented by experiments such as tensile test and friction test. After that simple modeling is modified by applying Bhatnagar’s model [7]. But it has a limit about fiber orientation. It is because the shear strength cannot be decided in all fiber orientations. For complementing this, modified model is supposed to be made by applying Zhang’s model [8]. This model can be solved in condition of all fiber orientations.

Force prediction model along all fiber orientations can be applied to predict damage zone in CFRP machining. After previous research, Delamination prediction model can be supposed to be developed including machining parameters such as feed rate and cutting speed as shown in **Fig.1-3**. This can be helpful for optimizing the machinability in CFRP machining. Developed models can also expand from orthogonal machining to the drill machining.

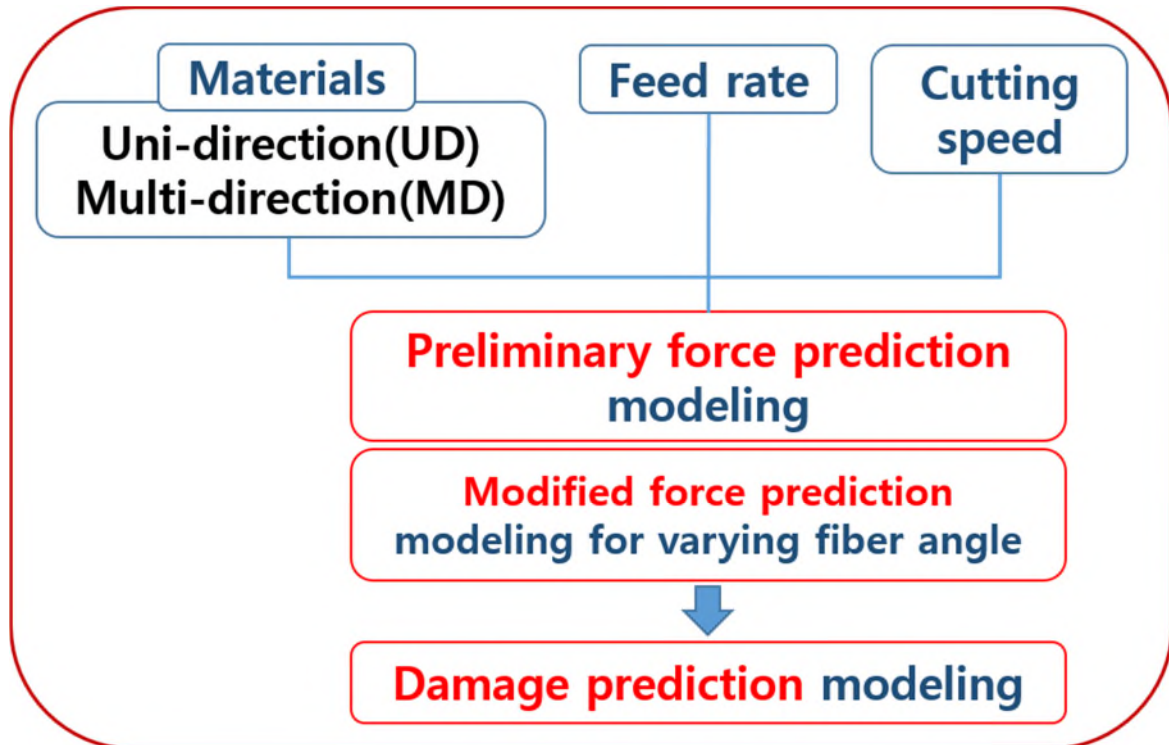


Fig. 1-3 Parameters and types of numerical modeling

1.3. Dissertation organization

This research is about the modified theoretical analysis of Carbon Fiber Reinforced Plastics (CFRP) machining. In this numerical modeling and experiment, it can be helpful to identify the properties of CFRP machining and increase reliability of numerical model by experimental validation.

For this goal, this study includes four steps:

Step 1: Determine CFRP properties by trying out tensile test and friction test.

Step 2: Develop force numerical prediction models.

Step 3: Experiment CFRP orthogonal cutting for identifying the force along the fiber orientations.

Step 4: Verify the results of numerical modeling compared to the experimental results.

Numerical modeling is for estimating the force and defects in CFRP machining. The objective of this thesis is to find optimal modeling for predicting the force generated by orthogonal cutting along the fiber orientation. Two models are supposed to be suggested, one for preliminary modeling and one for modified modeling for all the fiber orientations. **Fig. 1-4** shows overall modeling procedure in CFRP machining. Numerical modeling is affected by parameters as feed rate, cutting speed in machining and material's properties.

Force prediction modeling can also affect the defects prediction afterwards. Depending on the force prediction model, damage prediction model can be suggested. Lastly, force and damage prediction models are needed to be validated by experimental results along the fiber orientation and depending on the machining parameters. The objective of this study is to develop the numerical solution for force and damage prediction in CFRP machining and optimize CFRP machining for minimizing defects.

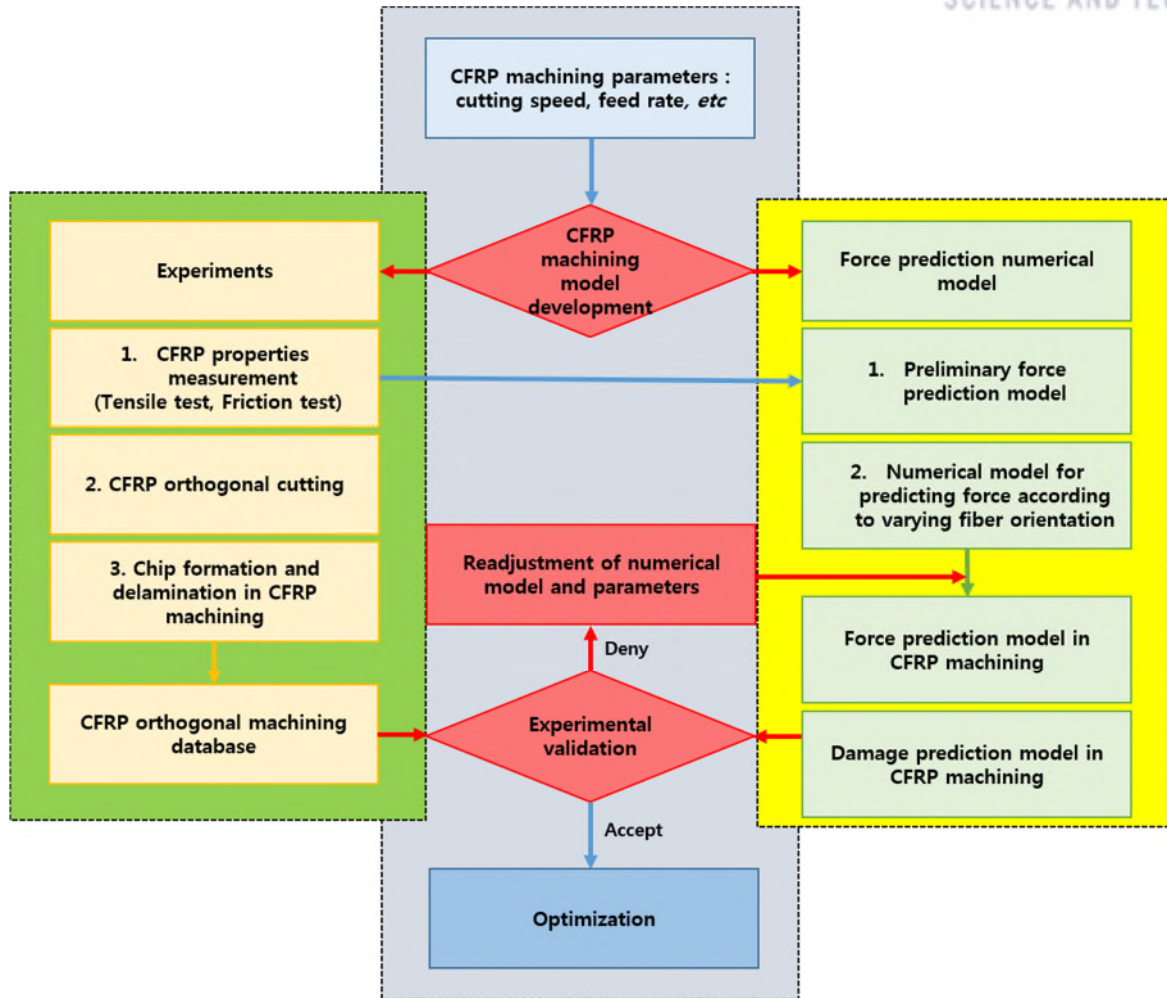


Fig. 1-4 Flow chart for the organization of the dissertation

2. Literature review

This literature review includes five main components:

- (1) Industrial applications of CFRP machining
- (2) Introduction of CFRP orthogonal cutting characteristics
- (3) Numerical modeling of CFRP machining
- (4) Flow of research about theoretical prediction model in CFRP machining

Literature review can help find out direction of this thesis. The history of research about CFRP machining is not long compared to metal cutting research's history. Therefore, complementing numerical modeling of CFRP machining by understanding material's property is essential to improve machinability.

2.1. Introduction of CFRP machining

As mentioned previously, CFRP has many advantages such as high strength to weight ratio, high stiffness and high corrosion resistance. Therefore, CFRP material is proper for many applications in engineering area. Today, CFRP is widely used in aerospace, automotive, and sports goods. Long time ago, in the late 1960s, it is used in the construction industry for the first time.



Fig. 2-1 The XXsys carbon fiber jacket site filament winding technique (USA) [9]

Fig. 2-1 representively shows main application as complement and reinforcement materials. The composite with high strength to weight ratio is proper to complement concrete. It is formed around the pillar of the bridge [9]. It can enhance durability. As shown in this application, forming and machining CFRP materials are inevitable to suit the different structures in each application.

In this thesis, we identify CFRP machining. There are representively three kinds of CFRP machining. First one is orthogonal cutting. It is defined as the workpiece forming process in 2 dimensional face [10]. It can occur the deformation in a single plane. In this process, fiber orientation is important point to decide machinability different from metal cutting as shown in **Fig. 2-2** [11]. As shown in **Fig. 2-2 (b)**, Fiber orientation angle is decided clockwise between feed way and fiber arrangement [12]. It can have advantages of identifying CFRP machining characteristics such as cutting forces, uncut and delamination along the fiber orientation.

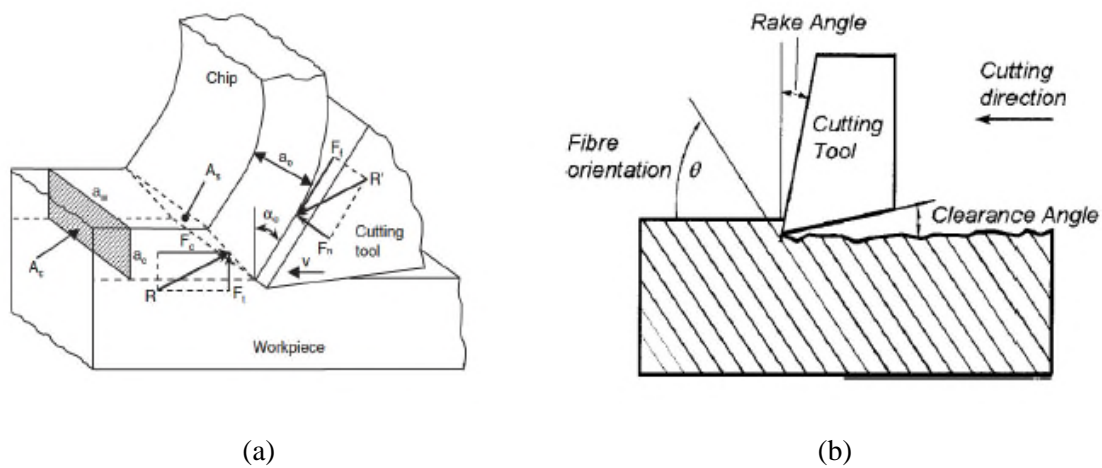


Fig. 2-2 Schematic of orthogonal cutting; (a) Metals, (b) UD-FRP [12]

Secondly, milling has some cutting edges of one tool which removes the workpiece. There are face milling and end milling in methods as **Fig. 2-3**. It has similar mechanism as CFRP orthogonal cutting. Cutting forces, uncut and delamination depends on the fiber orientation in CFRP milling [13-15].

Lastly, Drilling is the most common machining process in metal and composites cutting. It is called hole making process. It is considered as the workpiece forming procedure in 3 dimensional space. In **Fig. 2-4**, inlet and outlet of workpiece after CFRP drilling can be seen. Outlet of the workpiece has many defects such as uncut and delamination. It is affected by machining condition like feed rate and rotating speed. High feed rate and low rotating speed can make defects more with less machinability[16, 17]. This tendency can be also seen in other types of CFRP machining.

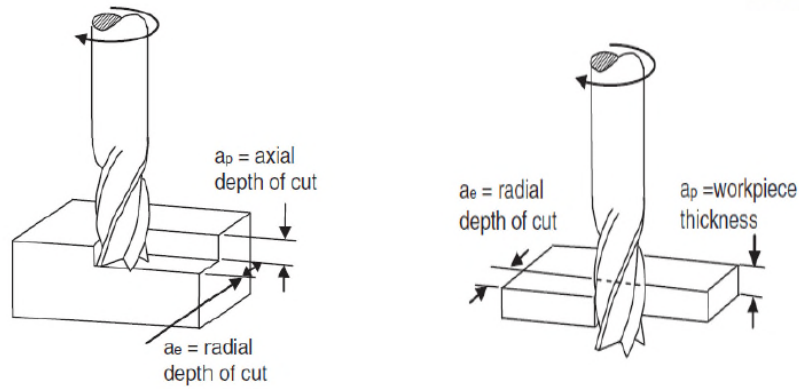


Fig. 2-3 Types of milling operations [18]

Entry				
Exit				
	Feed rate 64 μm/rev	Feed rate 320 μm/rev	Feed rate 64 μm/rev	Feed rate 320 μm/rev
	Cutting speed: 1500 rpm		Cutting speed: 6000 rpm	

Fig. 2-4 Machinability of CFRP drilling [19]

2.2. Characteristics in CFRP orthogonal machining

For fundamentally studying CFRP machining, orthogonal cutting is decided to identify. In this section, 4 factors are considered as key factors to decide machinability in CFRP orthogonal machining. There are (1) Force, (2) Chip formation, (3) Fiber orientation, (4) Delamination in CFRP orthogonal cutting. These factors are related to one another and they affect the machinability of CFRP machining.

2.2.1. Cutting forces in CFRP orthogonal machining

In CFRP orthogonal cutting, cutting forces are generated. The force generated along the feed direction is defined as cutting force along the fiber orientation [20]. And the force generated perpendicular to the feed direction and along the depth of cut is called thrust force. Metal cutting has smooth change of the cutting forces. On the other hand, there are many fluctuations of cutting forces change in CFRP orthogonal machining as shown in **Fig. 2-5** [12]. This tendency is because each fiber in CFRP materials is cut off when the tool goes through the workpiece. From this force data, we can get the mechanism of CFRP machining different from metal cutting.

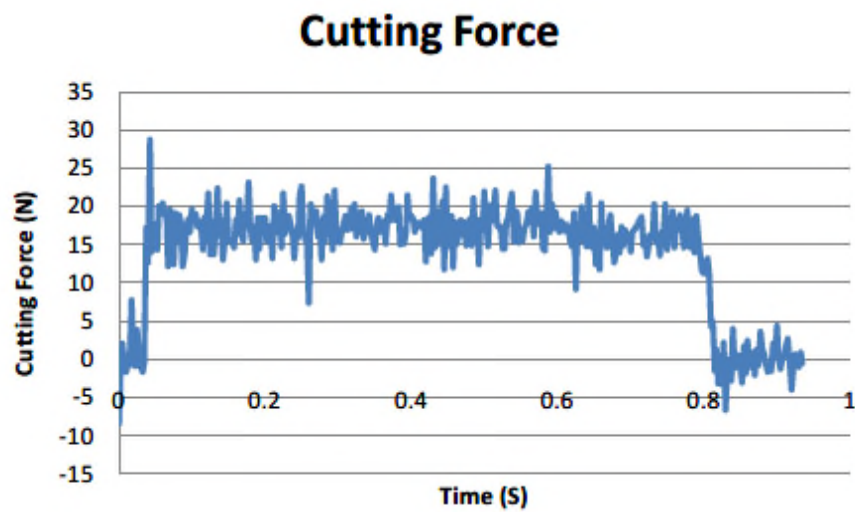


Fig. 2-5 Cutting force diagram in CFRP orthogonal cutting [12]

2.2.2. Fiber orientation in CFRP orthogonal machining

In manufacturing CFRP, aligned carbon fiber is synthesized with resin such as epoxy. So, CFRP has fiber orientation angle in each layer. As shown in **Fig. 2-6**, fiber orientation changes according to the tool feed direction in CFRP orthogonal cutting. It can affect cutting mechanism, force change and delamination [21-24].

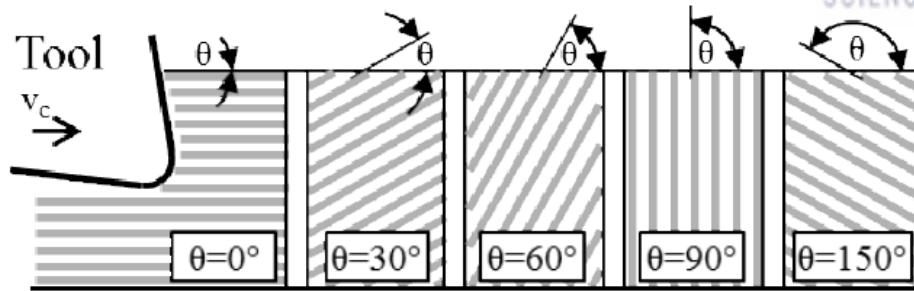
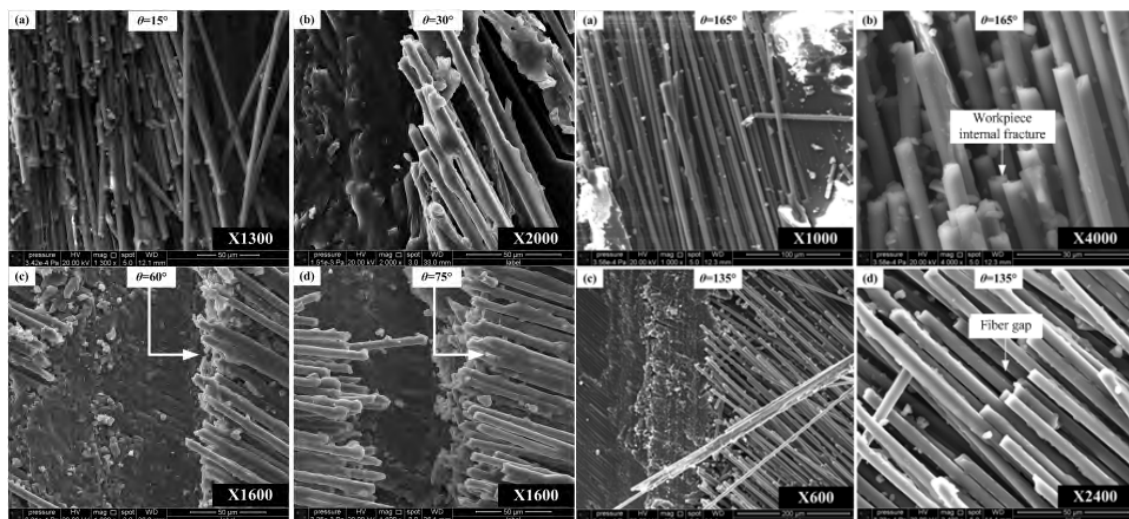


Fig. 2-6 Fiber orientation relative to the cutting direction [22]

2.2.3. Chip formation in CFRP orthogonal machining

Chip formation is important factor to find out mechanism of CFRP machining and estimate the machinability. It can help optimize the system in CFRP machining. The chip formation of CFRP machining is different from the metal cutting. The chip formation is usually continuous in metal cutting, however the chip formation of composites is discontinuous and the chip is type of dust. Therefore, it is difficult point to analyze CFRP machining. By using Scanning Electron Microscope (SEM), chip morphology can be seen as Fig. 2-7. In the range of fiber orientation, $0^\circ \leq \theta < 90^\circ$, the chip morphology is relatively smooth surface. There is little crack on the surface of the fibers. On the other hand, we can see rough surface of the fibers and the chips crash down in the range of fiber orientation, $90^\circ \leq \theta < 180^\circ$.



(a)

(b)

Fig. 2-7 Chip morphology SEM photos of carbon fiber with orientation angles along the fiber direction; (a) $0^\circ \leq \theta < 90^\circ$ fiber orientation, (b) $90^\circ \leq \theta < 180^\circ$ fiber orientation [25]

2.2.4. Delamination in CFRP orthogonal machining

Delamination is damage zone of composite materials where layers are split. Repeated cyclic stresses by the force change and impact can cause this defects in CFRP machining. In CFRP orthogonal cutting, Separate layers can cause significantly decreasing mechanical toughness and durability. Delamination can be also the reason of reinforcement corrosion. It can occur oxidation of reinforcement [26, 27]. Most defects is generally occurred in the fiber orientation over 90° as shown in **Fig.2-8**. This result can be identified by numerical solution and experimental validation. In this damage prediction model [28], there is input parameter of force. Actually, there are many researches about numerical force prediction model but there is few theoretical force prediction models in the range of the fiber orientation over 90° . For predicting the damage zone, numerical force prediction model in the range of the fiber angle over 90° is essential. This research has an importance to enhance the machinability of CFRP machining.

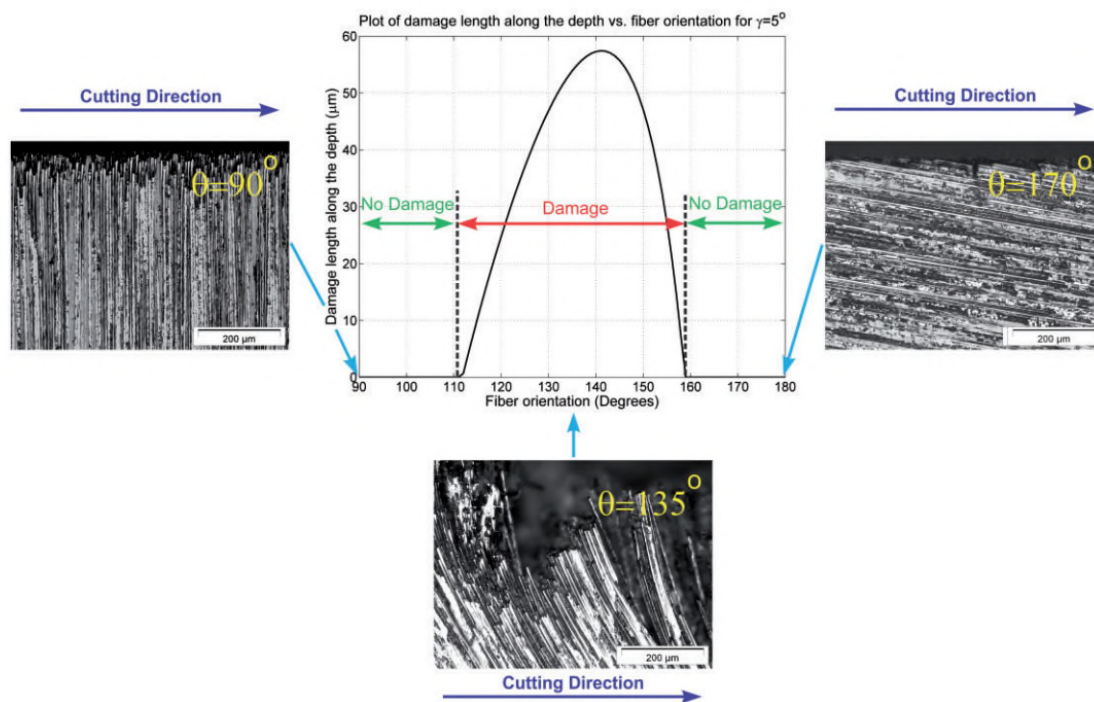


Fig. 2-8 Comparison of experimental and analytical results for predicting damage [28]

2.3. Numerical solutions to predict force in CFRP machining

In this study, identifying CFRP orthogonal cutting is important because it can show force change along the fiber orientation according to the feed rate and cutting speed. To predict the force in CFRP orthogonal cutting, there are 3 kinds of numerical solutions.

First one is theoretical model. Only a few researchers have tried to analyze theoretical solution for predicting force from the mechanics of chip formation by (Takeyama et al., 1988 [29]; Bhatnagar et al., 1995 [7]; Zhang et al., 2001 [8]). It has many advantages of short time consumed when simulating and it can be identified by cutting mechanism. On the other hand, it is inevitable to adjust many assumptions.

Secondly, there is experimental numerical model to predict force by (Jamal et al., 2008 [18]). Experimental numerical model has advantages of high accuracy compared to other methods with experimental parameters, K_c, K_t . However, it needs preliminary experimental results and it has possibility of getting different results depending on conditions.

Lastly, Finite Element Method (FEM) is good for identifying CFRP cutting process in CFRP orthogonal machining. It can show the predicted failure modes identified for different fiber orientation angle by (Abena et al., 2015 [30]). It has good point about visualization and showing chip formation predicted. Its limit is sometimes too much time needed and different results depending on the computers.

These numerical methods are inevitable to be verified by CFRP machining results such as cutting force and thrust force. Representatively, CFRP orthogonal machining is the most effective to find out the relationship between cutting forces and fiber orientation angle. In this process, numerical prediction model has become more accurate.

These numerical force prediction models are important to define characteristics of CFRP machining and achieve optimization of machinability in each machining parameters such as feed rate and depth of cut in CFRP machining. As mentioned previously, especially in theoretical damage prediction model [28], there is input parameter of force which is not defined yet. So we have an effort to establish theoretical model which predicts force in the range of all the fiber orientation from 0° to 90° .

2.4. Flow of research about theoretical solution to predict force and delamination in CFRP machining

The machinability of CFRP machining is associated with the chip formation along the fiber orientation [31-34]. For identifying theoretical force prediction model, it is essential to understand

chip formation. There are many researches about chip formation. Firstly, this study was reported by Koplev. And he showed a micrograph of two specimens in 1983 [35]. One is machined perpendicular to fiber orientation angle. And the other is parallel to the fiber orientation as shown in **Fig.2-9**.

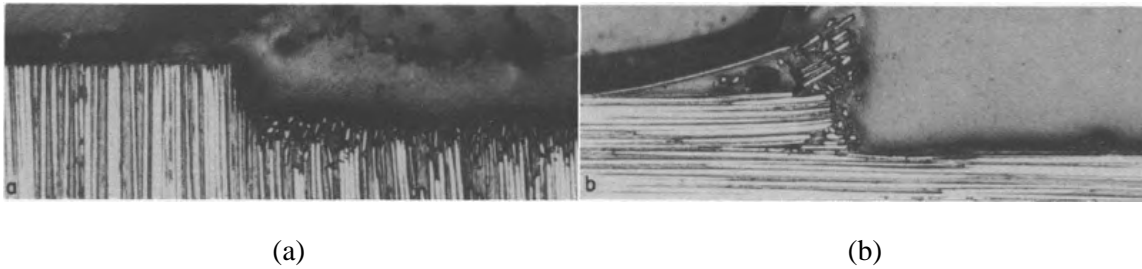


Fig. 2-9 Cross section of specimens in CFRP cutting; (a) fiber angle 90° , (b) 0° [35]

Afterward, diverse fiber orientation has been researched in composite machining. D. H. Wang suggested the cutting mechanism by diverse fiber orientation in composite orthogonal cutting shown in **Fig. 2-10** [36], representatively.

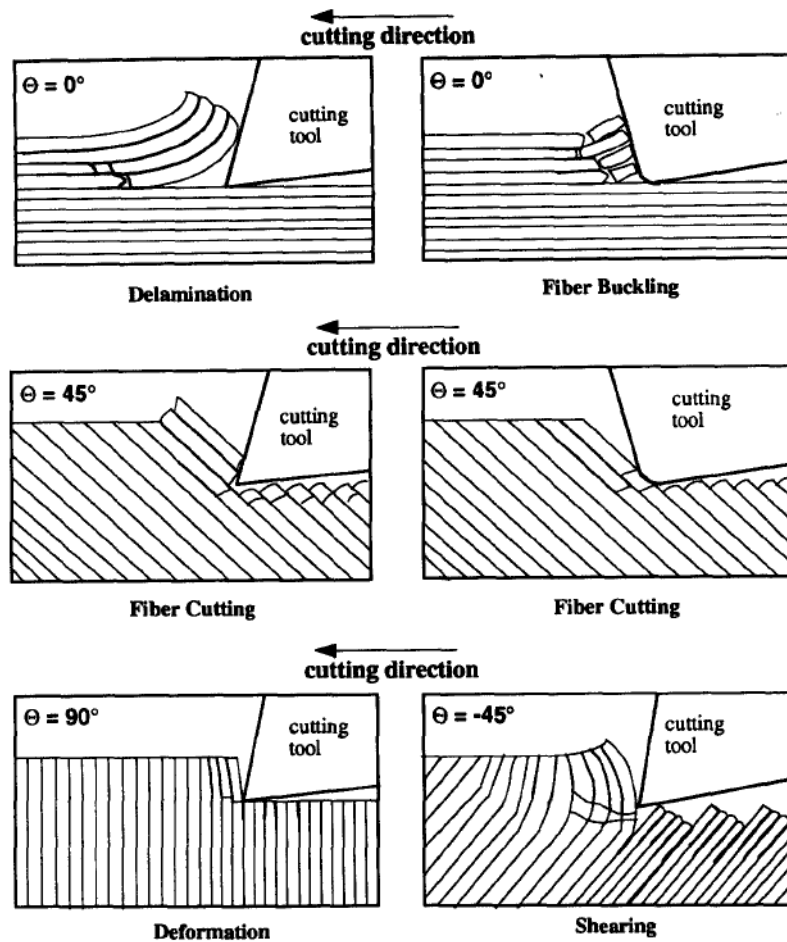


Fig. 2-10 Cutting mechanisms in the orthogonal machining of composite [36]

In the fiber orientation below 90° , fiber is cut by cutting tool. In the fiber orientation angle over 90° , it occurs fiber bending, delamination and shearing. It can generate defects. High thrust force can be generated by elastic recovery of the fibers critically in fiber orientation below 90° .

For identifying machinability of CFRP cutting, it is principal to predict damage zone along the fiber orientation in each machining condition. It is necessary to find out machinability especially in fiber orientation over 90° . X. M. Wang and L. C. Zhang observed the microstructure concentrating the range of fiber orientation over 90° as shown in **Fig. 2-11** [37].

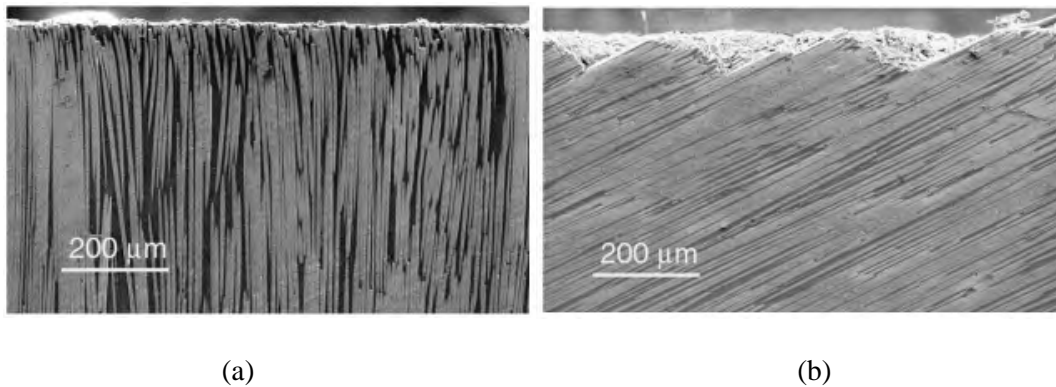


Fig. 2-11 Cross section of specimens in CFRP cutting; (a) fiber angle 90° , (b) 180° [37]

These chip formation researches can help understand cutting mechanism and establish numerical force prediction model. Takeyama and Iijima (1988) proposed chip formation in composite machining can be affected by shearing the composite along the shear plane with shear angle, ϕ as shown in **Fig. 2-12** [29].

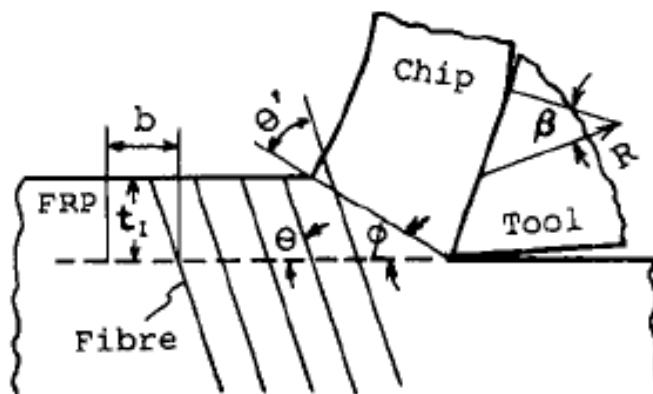


Fig. 2-12 Orthogonal cutting model of composite [29]

ϕ : Shear angle, θ : Fiber angle, θ' : Shear fiber angle

In this model, Merchant's theory of minimum cutting energy determine the shear plane angle, ϕ . And the shearing stress in the shear plane is only a function of fiber orientation angle, θ . The fiber orientation angle, θ is limited as less than 90° . This type of cut is 2 dimensional. The effect of temperature can be ignored. Shearing the composite occur in the condition of minimizing the cutting energy.

In Bhatnagar's model (1995), it was assumed that the chip flow in UD CFRP machining is almost equal to the plane of the fiber [7]. It means, the shear plane angle, ϕ coincides with the fiber orientation angle, θ . In this model, direction definition of fiber angle, θ is reverse that is different from other thesis. It is also assumed that this model is reasonable in the range of the fiber orientation over 90° . In addition, the Iosipescu shear test was implemented to get the in-plane shear strength for CFRP. The shearing stress in the shear plane is only a function of fiber angle, θ .

L. C. Zhang (2001) suggested mechanics model base on the observations of CFRP orthogonal cutting with cutting tool nose radius [8]. According to this model, the cutting zone is divided in 3 regions shown in **Fig. 2-13**.

Firstly in Region 1, cutting forces are generated by chip along the rake face of the cutting tool. This chipping region includes the material subjected to shearing along the shear plane. This region contains the actual depth of cut, a_c . So, this region is important to consider machining parameter such as feed rate in numerical solution. However, the amount of the cutting forces in this region is not big compared to metal cutting. It is because the chip is continuous in metal cutting. On the other hand, the chip is just dust type in CFRP machining.

Secondly in Region 2, cutting forces are occurred by the indentation force in tool nose radius. It is round edge of the tool. Tool nose is pressing the fiber. This force can be most significant in resultant force.

Lastly in Region 3, Cutting forces are generated under the tool in CFRP machining. Bouncing of the fiber in CFRP workpiece can affect cutting forces because fiber has elastic properties under the tool.

Finally, this thesis identifies validation of numerical solution by comparing with experimental results when depth of cut and fiber orientation change. This material is MTM56 and the effective modulus in Region 3, E_3 is 5.5GPa. This specimen thickness is 4mm. This comparison can be seen in **Fig. 2-14 (a)**. We follow this thesis by using MATLAB code. This result is shown in **Fig. 2-13 (b)**.

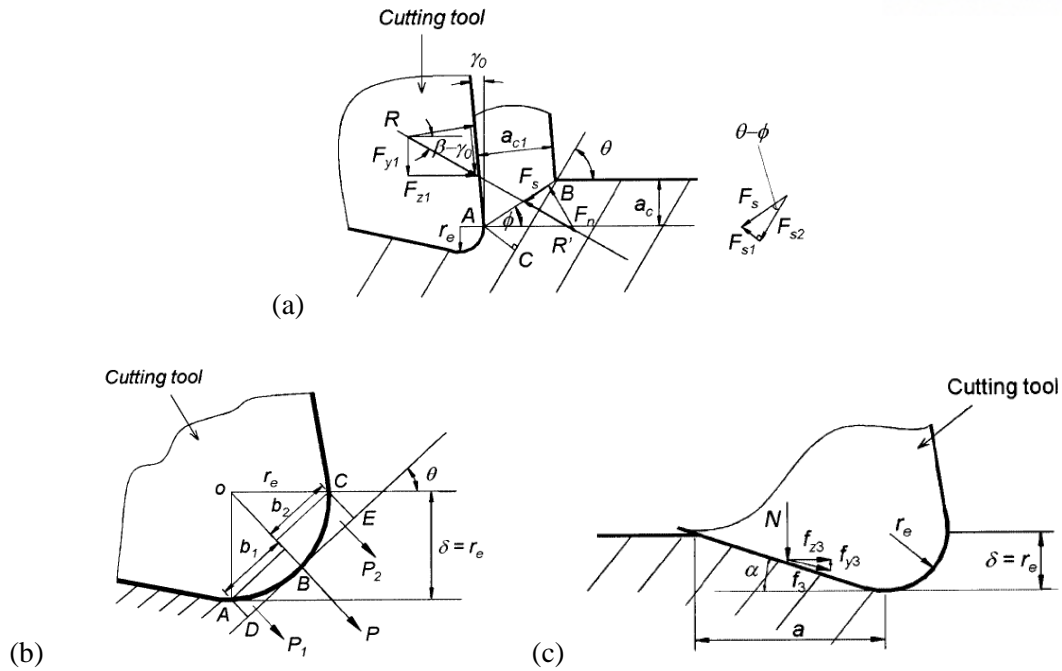


Fig. 2-13 The cutting diagram in CFRP orthogonal machining; (a) Region 1, (b) Region 2, and (c) Region 3 [8]

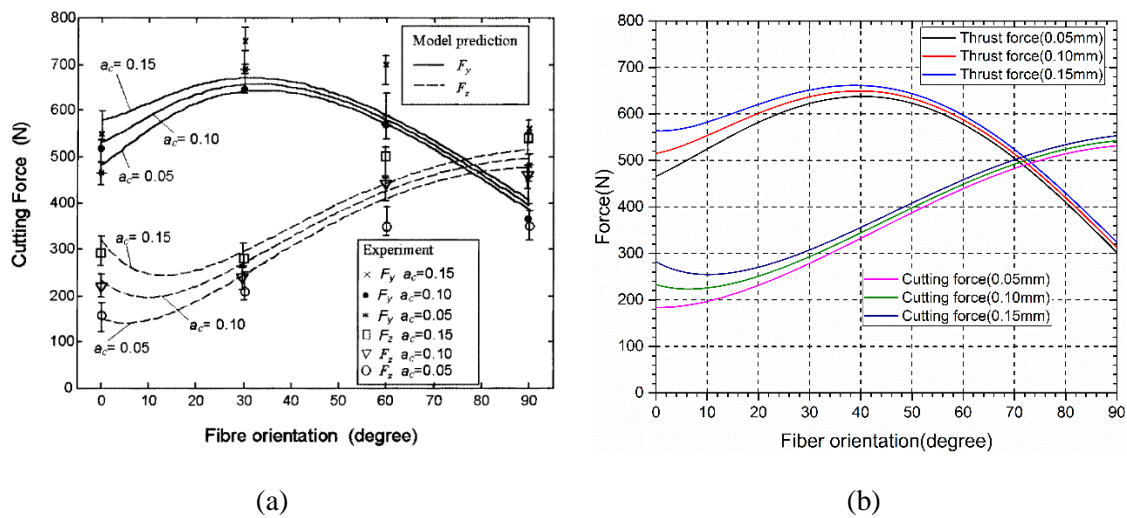


Fig. 2-14 Comparison between numerical model predictions and experimental results of MTM56 in (a) thesis [8], (b) using MATLAB code

In this research area, there are many other models which is from microstructure of fiber and micro-buckling of fiber in CFRP. Jaromi suggested micro-buckling of the fiber as shown in **Fig. 2-15** [38]. Qi's model [39] was based on deflection function of Representative Volume Element (RVE) and it

concentrates on micro-deflection similar to Jaromi’s model. And Chen recently also find out micro-deflection and micro-buckling of fiber [40].

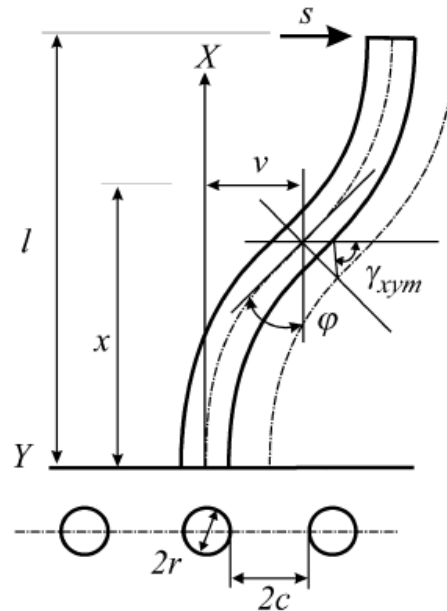


Fig. 2-15 Schematic of a single fiber under lateral force [38]

These models are not modeling of the chip formation. However, this model has limit of low accuracy and complicated parameters to get such as fiber volume fraction, v_f , fiber spacing, c , and shear strain of matrix, γ . Therefore, this study is supposed to adopt theoretical force prediction model from chip formation in CFRR machining.

However, these researches have limit which is only the case of low speed machining. Actually, Koplev had the condition of 14m/min cutting speed [35], D. H. Wang did experiment with 4, 9, 14m/min [36], and X. M. Wang had the cutting speed of 1m/min. In addition Takeyama’s cutting speed condition is 0.38mm/min [37]. Bhatnagar’s cutting speed condition is 1.18m/min [7], and L. C. Zhang [8] has condition of 1m/min. all the researches are about low speed machining. In this study, we can find out difference in other condition such as high speed machining.

Except to the other models from micro-buckling which has low accuracy and complicated parameters to get, numerical force prediction models from the chip formation have the limit of predicting only in the range of fiber orientation below 90° . And we need to find out force prediction model for predicting this damage zone and estimating machinability. As mentioned previously, most defects are occurred in the fiber orientation over 90° . This is also mentioned in Zhang’s study as shown in **Fig. 2-16** [8]. Therefore, we have an effort to expand the original model to all the fiber orientations in theoretical approach from the chip formation in this study.



Fig. 2-16 Effect of fiber orientation in surface roughness [8]

For this objective, we decide to apply Bhatnagar’s model and L. C. Zhang’s model into preliminary model and numerical model for predicting force according to varying fiber orientation. Preliminary model can include MD CFRP material and enhance the accuracy of predicting force. Modified model can identify the force change in the fiber orientation from 0° to 180°.

3. Numerical modeling

3.1. Numerical model for predicting force

In this section, force prediction numerical models are introduced. The first one is preliminary model for predicting force. Its reference is Bhatnagar’s force prediction model [7]. This model has a condition of fiber orientation, $\theta < 90^\circ$ and Uni-direction (UD) CFRP. In this condition, it is possible to assume shear angle is equal to the fiber orientation. From this model, modified model is developed to consider Multi-direction (MD) CFRP and Epoxy region.

The second is numerical model for predicting force according to varying fiber orientation. It would be helpful to complement the first introduced model because change of the force can be detected continuously as the fiber orientation changes. This original model is Zhang LC’s model [8]. This model has a condition of fiber orientation, $\theta < 90^\circ$. This research can expand this model to the model along all range of the fiber orientation, $0^\circ \leq \theta < 180^\circ$. This research has an importance to enhance the machinability of CFRP machining by putting this model into damage prediction model.

3.1.1. Preliminary model for predicting force

Orthogonal cutting is representative of two-dimensional cutting. Therefore, we can identify the characteristics affected by fiber orientation. In this procedure, horizontal force and vertical force are occurred as shown in **Fig. 3-1**.

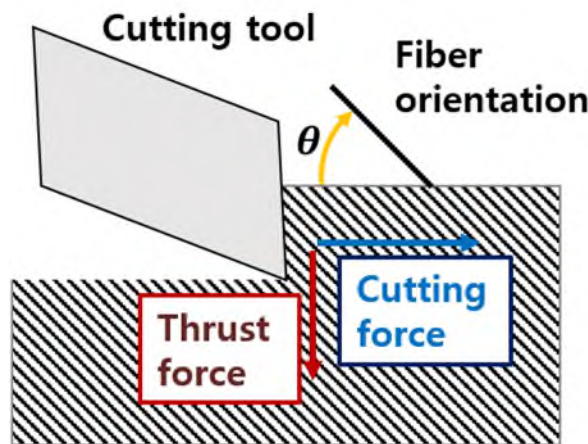


Fig. 3-1 Schematic of CFRP orthogonal cutting

It can help identify the characteristics of CFRP machining. For estimating the force by numerical solution in CFRP orthogonal machining, Bhatnagar's force numerical model is considered fundamentally [7].

Original Bhatnagar's force prediction model considers the chip flow in machining unidirectional FRPs. This model is suggested as (3-1) and (3-2).

$$F_c = \frac{\tau_0 A_0 \cos(\beta_0 - \gamma)}{\sin\theta \cos(\theta + \beta_0 - \gamma)} \quad (3-3)$$

$$F_t = \frac{\tau_0 A_0 \sin(\beta_0 - \gamma)}{\sin\theta \cos(\theta + \beta_0 - \gamma)} \quad (3-4)$$

In these equations, F_c and F_t are the cutting force and the thrust force respectively, τ_0 is the shear strength along the fiber orientation, A_0 is the area of composite's undeformed chip area, β_0 is the composite's friction angle, and γ means the rake angle of the tool.

New model is modified to consider Multi-direction (MD) CFRP and Epoxy in matrix because Bhatnagar's force numerical model is only applied to Uni-direction (UD) CFRP. This model is as shown in (3-3) and (3-4). This model is only applied in case of fiber orientation, $\theta < 90^\circ$. In this condition, shear angle, ϕ is assumed to be fiber orientation, θ . It is related to the chip formation along the fiber orientation. Lastly, epoxy's chip formation is suggested to be similar to the fiber chip formation.

$$F_c = \tau_0 \left(\frac{A_1 \cos(\beta_1 - \gamma)}{\sin\theta \cos(\theta + \beta_1 - \gamma)} + \frac{A_2 \cos(\beta_2 - \gamma)}{\sin\theta \cos(\theta + \beta_2 - \gamma)} \right) \quad (3-3)$$

$$F_t = \tau_0 \left(\frac{A_1 \sin(\beta_1 - \gamma)}{\sin\theta \cos(\theta + \beta_1 - \gamma)} + \frac{A_2 \sin(\beta_2 - \gamma)}{\sin\theta \cos(\theta + \beta_2 - \gamma)} \right) \quad (3-4)$$

In these equations, F_c and F_t are the cutting force and the thrust force respectively, τ_0 is the shear strength along the fiber orientation, A_1 is the area of fiber's undeformed chip area, A_2 is the area of epoxy's undeformed chip area, β_1 is the fiber's friction angle, β_2 is the epoxy's friction angle, and γ means the rake angle.

3.1.2. Numerical model for predicting force according to varying fiber orientation

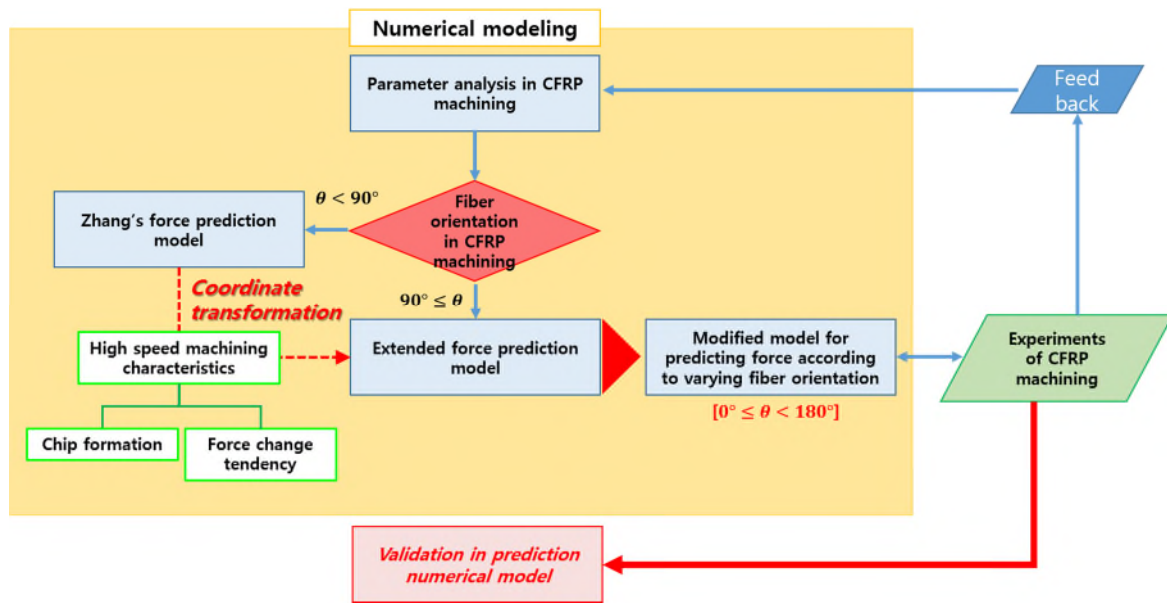


Fig. 3-2 Flow chart for force prediction model according to varying fiber orientation

In the preliminary model for predicting force, there are some limits that it is only applied to the fiber orientation, $\theta > 90^\circ$ and discontinuous model. In this study, other approach model is suggested by understating and complementing previous models. This research can expand Zhang's model to the model depending on all the range of the fiber orientation, $0^\circ \leq \theta < 180^\circ$. This research has an importance to enhance the machinability of CFRP machining by applying this model into damage prediction model. This force prediction model suggests three distinct regions in the deformation mechanisms of CFRP machining as shown in **Fig. 3-3**. This model was first represented by Zhang [8].

Region 1 has a depth of cut, a_c . In the region 1, chipping is generated by CFRP cutting along the tool's upper side. In this region, similar mechanism can be seen as section 3.1.1. Preliminary model for predicting force. Region 2 covers the area of tool nose. We consider Region 2 is the most effective region because the chipping in Region 1 is just dust type. It's not continuous chip like metal cutting. It means, chipping is not effective in CFRP machining. Region 3 is where composite bouncing is occurred in the region of the lowest area of the tool.

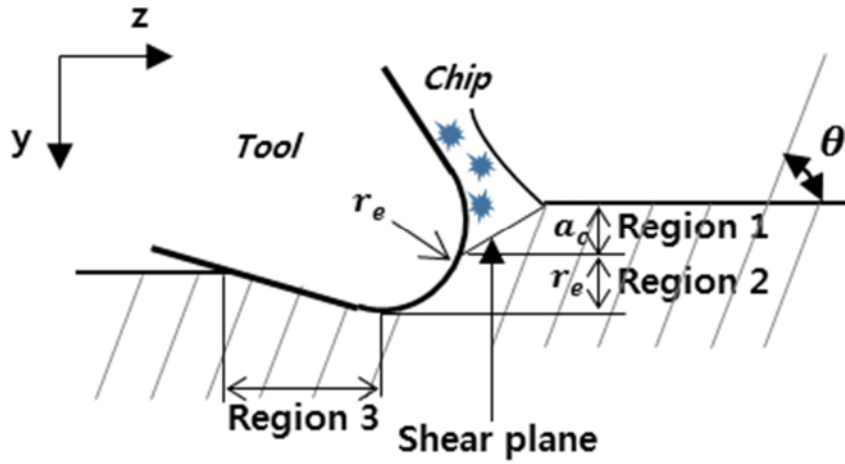


Fig. 3-3 Schematic of CFRP orthogonal cutting

3.1.2.1. Region 1 – Chipping

In region 1, chipping occur in the process with sharp cutting tool. In **Fig. 3-4**, there is theoretical shear plane formed when fracture of fibers occurs. As shown in this figure, Chipping would be generating the cutting force and thrust force. This chipping region is important because it contains machining parameter such as feed rate.

The effects along the depth of cut which is affected by feed rate are shown only in this region. These specific equations are as shown in (3-5) and (3-6). (3-5) is along the cutting direction and (3-6) is along the thrust direction.

$$F_{z1} = \frac{\tau_1 h a_c (\sin\phi \tan(\phi + \beta - \gamma) + \cos\phi)}{\frac{\tau_1}{\tau_2} \cos(\theta - \phi) \sin\theta - \sin(\theta - \phi) \cos\theta} \quad (3-5)$$

$$F_{y1} = \frac{\tau_1 h a_c (\cos\phi \tan(\phi + \beta - \gamma) - \sin\phi)}{\frac{\tau_1}{\tau_2} \cos(\theta - \phi) \sin\theta - \sin(\theta - \phi) \cos\theta} \quad (3-6)$$

In these equations, F_{z1} and F_{y1} are the cutting force and the thrust force respectively in region 1, τ_1 is the shear strength along the fiber orientation, τ_2 is the shear strength along the direction normal to fiber orientation. h is the width of a workpiece, a_c is the depth of cut in machining, ϕ is the shear angle, β is the friction angle, γ means the rake angle of a cutting tool, and θ is fiber

orientation.

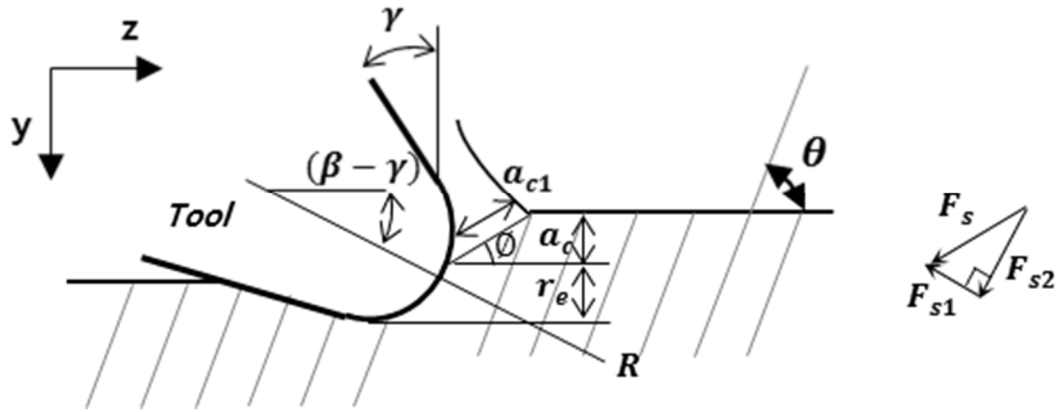


Fig. 3-4 Schematic of CFRP orthogonal cutting in Region 1

For calculating these force equations, ϕ needs to be found. Following the general cutting mechanics, (3-7) and (3-8) are suggested.

$$\tan\phi = \frac{r_c \cos\gamma}{1 - \sin\gamma} \quad (3-7)$$

$$r_c = \frac{a_c}{a_{c1}} \quad (3-8)$$

In this equation, a_{c1} is the chip thickness. CFRP is a typical brittle material in machining. In this reason, it could be assumed that r_c is 1. Therefore, It is determined by (3-9).

$$\phi \approx \tan^{-1} \left(\frac{\cos\gamma}{1 - \sin\gamma} \right) \quad (3-9)$$

3.1.2.2. Region 2 – Pressing

Fig. 3-5 show how to analyze cutting mechanism in Region 2. In Region 2, the force is caused

from the tool nose. Tool nose presses the workpiece and it is generating the deformation. It seems like the process of generating plowing force. In CFRP, these indentation forces are affected by the fiber orientation, θ .

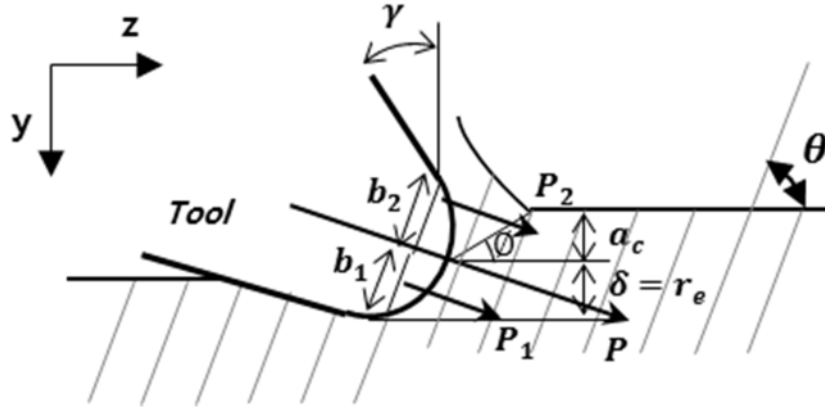


Fig. 3-5 Schematic of CFRP orthogonal cutting in Region 2

As shown in **Fig. 3-5**, the indentation forces are calculated by adding the force generated in upper tool nose and the other force generated in lower tool nose. These specific equations about indentation forces in Region 2 are shown in (3-10) and (3-11).

$$P_1 = \frac{\frac{1}{2}b_1^2\pi E^* h}{4r_e} \quad (3-10)$$

$$P_2 = \frac{\frac{1}{2}b_2^2\pi E^* h}{4r_e} \quad (3-11)$$

In these equations, P_1 and P_2 represent indentation forces in the direction normal to the fiber orientation. E^* is the effective elastic modulus of CFRP material along the P_1 and P_2 direction. h is the width of the workpiece, r_e is the tool nose radius. b_1 and b_2 are the widths of the contact between tool and workpiece.

b_1 and b_2 can be calculated as (3-12) and (3-13).

$$b_1 = r_e \sin \theta \quad (3-12)$$

$$b_2 = r_e \cos \theta \quad (3-13)$$

The effective elastic modulus E^* is defined by (3-14).

$$E^* = \frac{E}{1-\nu^2} \quad (3-14)$$

Where, E is Young's modulus of CFRP material along the P_1 and P_2 direction. ν is the minor Poisson's ratio. Therefore, the resultant force is $P = P_1 + P_2$. Finally, the total cutting force and thrust force in Region 2 is determined as (3-15) and (3-16).

$$F_{z2} = P_{real}(\cos\theta + \mu\sin\theta) \quad (3-15)$$

$$F_{y2} = P_{real}(\sin\theta - \mu\cos\theta) \quad (3-16)$$

In these equations, F_{z2} and F_{y2} are the cutting force and the thrust force respectively in Region 2, P_{real} is $K(f) * P$ in which, $K(f)$ is a factor related to the fiber orientation. It is function of fiber orientation to be determined by experiment. μ is the friction coefficient.

3.1.2.3. Region 3 – Bouncing

In Region 3, the tool is caused by the workpiece material bouncing in the clearance face. **Fig. 3-6** shows the cutting mechanism in region 3.

For calculating simply, the bouncing is complete is assumed. In this condition, the bouncing back height is same as the radius of tool, r_e . The contact length along the clearance face is $a = \frac{r_e}{\tan\alpha}$ as shown in **Fig. 3-6**.

$$F_{z3} = \frac{1}{2}r_e E_3 h \cos^2 \alpha \quad (3-17)$$

$$F_{y3} = \frac{1}{2}r_e E_3 h (1 - \mu \cos \alpha \sin \alpha) \quad (3-18)$$

In these equations, F_{z3} and F_{y3} are the cutting force and the thrust force respectively in Region 3, E_3 is the effective modulus of the materials in Region 3. α is the clearance angle.

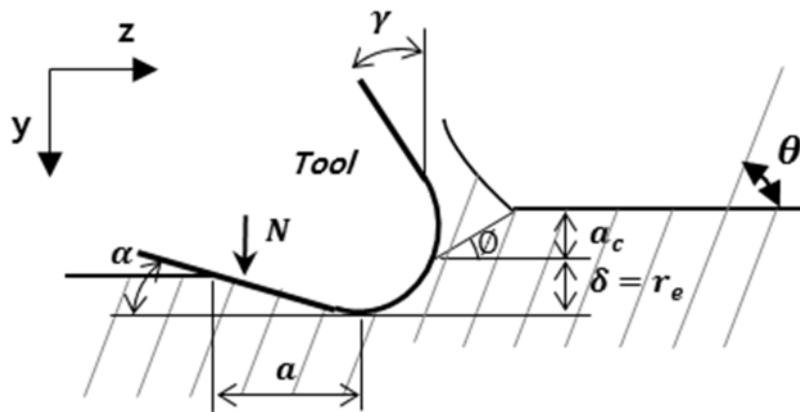


Fig. 3-6 Schematic of CFRP orthogonal cutting in Region 3

3.1.2.4. The total cutting forces

The sum of the cutting forces and the thrust forces each is the total forces.

$$F_z = F_{z1} + F_{z2} + F_{z3} \quad (3-19)$$

$$F_y = F_{y1} + F_{y2} + F_{y3} \quad (3-20)$$

In these equations (3-12) and (3-13), F_z and F_y are total cutting force and total thrust force respectively in case of fiber orientation, $\theta < 90^\circ$. In low speed machining, fiber bending occurred

in case of fiber orientation, $\theta > 90^\circ$. It needs other mechanisms for this. On the other hand, no fiber bending occurred in case of fiber orientation, $\theta > 90^\circ$ in high speed machining. We can also get the evidence of this assumption from chip formation in CFRP orthogonal machining also for experimental validation in Chapter 4. In this research, it considers the high speed machining (Cutting speed $> 80\text{m/min}$). Therefore, it is considered to put $(180^\circ - \theta)$ into this model instead of θ in case of fiber orientation, $\theta > 90^\circ$.

3.2. Numerical model for predicting damage

In this section, damage prediction numerical model is applied from the force prediction model. As discussed previously, previously mentioned force prediction model according to varying fiber orientation is suggested to be applied as shown in **Fig. 3-7**. This can help estimate machinability along all the fiber orientations and find out optimized machining conditions.

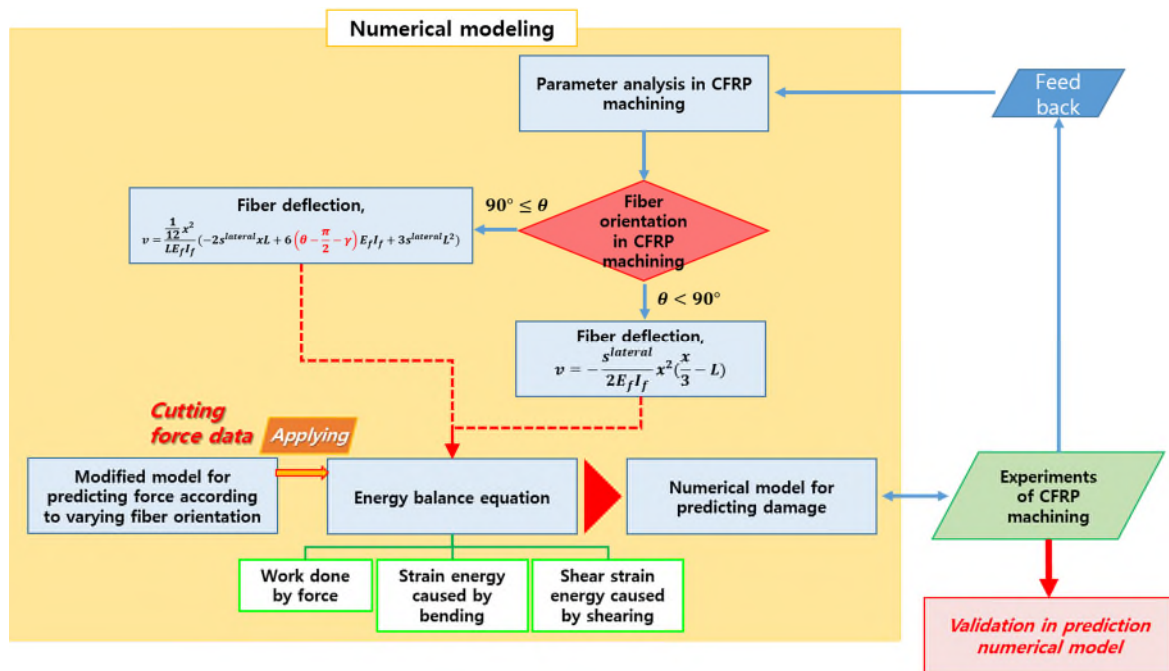


Fig. 3-7 Flow chart for showing the organization of damage prediction model

Damage prediction model suggests micro-scale analysis in the deformation mechanisms of CFRP machining as shown in **Fig. 3-8**. In **Fig. 3-8**, γ_{matrix} is the shear strain in the matrix material, $2c$ is fiber spacing and r means fiber’s radius. This model was first represented by Jahromi [28]. This

analysis is followed by a few assumptions. It is 2-dimensional deformation. Fiber has no shear and matrix material has no compression or extension. Normal stress in fiber is negligible. Tool nose radius is assumed to be zero.

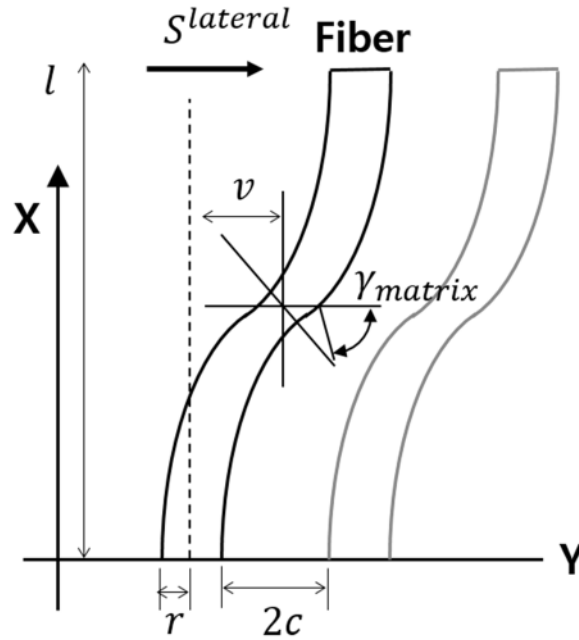


Fig. 3-8 Schematic of micro-scale cutting mechanism in CFRP machining

In this study, we use energy balance theory. This theory is applied in a situation that a single fiber is surrounded by matrix material. Total energy can be shown mathematically as (3-21). First term is the work exerted by the external force, $S^{lateral}$. Second term is strain energy of the fiber influenced by the external force. And last term is the shear strain energy of matrix material.

$$U = - \int_0^L S^{lateral} \left(\frac{dv}{dx} \right) dx + \frac{1}{2} \int_0^L E_f I_f \left(\frac{d^2v}{dx^2} \right)^2 dx + A_m \left(- \frac{L\tau_c^2}{2G_m} + \tau_c \left(1 + \frac{r}{c} \right) \int_0^L \frac{dv}{dx} dx \right) = 0 \quad (3-21)$$

In this equation (3-21), U is the total energy, v is the deflection of a fiber, E_f is fiber's elastic modulus, I_f is fiber's second moment of area, A_m is matrix area, G_m is matrix's shear modulus, τ_c is matrix's shear strength and L is length of reinforcement. In this equation, we define the external force in a single fiber, $S^{lateral}$ as (3-22). H is total width of workpiece and F_c is cutting force calculated from previous force prediction model.

$$S^{lateral} = F_c \left(\frac{2r}{H} \right) \quad (3-22)$$

According to fiber orientation, there are two cases of cutting mechanism. If the fiber orientation is less than 90° , tool push fiber's face and fiber is cut. If the fiber orientation is bigger than 90° , fibers can be tangent to the tool rake side and they break. Therefore, each case has different boundary conditions.

After applying boundary conditions in the range of fiber orientation less than 90° , the fiber deflection, v can be shown as (3-23). In the range of fiber orientation bigger than 90° , the fiber deflection, v can be shown as (3-24). In this equation, θ is fiber orientation and γ is rake angle of the tool.

$$v = -\frac{S^{lateral}}{2E_f I_f} x^2 \left(\frac{x}{3} - L \right) \quad (3-23)$$

$$v = \frac{1}{12} \left(\frac{x^2}{LE_f I_f} \right) \left(-2 S^{lateral} xL + 6 \left(\theta - \frac{\pi}{2} - \gamma \right) E_f I_f + 3 S^{lateral} L^2 \right) \quad (3-24)$$

In the last, L values calculated from energy balance equation should be the damage length along the fiber direction. Damage length along the fiber direction needs to change over to damage length along the depth. $(L * \sin\theta - a_c)$ is damage length along the depth. a_c is depth of cut. If $(L * \sin\theta)$ is less than depth of cut, a_c , there is no damage in applicable condition. In the opposite case, there is damage occurred.

4. Experimental validation

4.1. Experimental validation of preliminary model for predicting force

In this section, it is considered that fiber angle direction is reverse to original definition of other thesis. It means, fiber angle, $(180^\circ - \theta)$ in this model is actually applied to original definition of fiber orientation, θ as previously mentioned in **Fig. 3-2**.

4.1.1. MD CFRP property test

In this section, MD CFRP is used to validate preliminary numerical model. So we need to identify its shear strength along the fiber orientation angle and friction angle from friction coefficient of MD CFRP. In this purpose, we did tensile test and friction test of MD CFRP.

4.1.1.1. Tensile test

MD CFRP workpieces are prepared for each fiber orientation of 20° , 40° , 60° . This fiber orientation is based on the surface outside of both directions. Tensile test equipment is INSTRON 5982 model. Each workpiece is fixed by upper and downer vise as shown in **Fig. 4-1**. The strain rate condition is 1mm/min in tensile direction. It is because CFRP is tendency to be brittle.

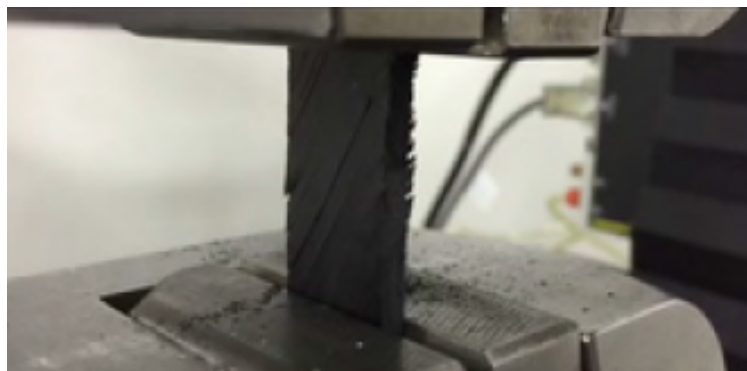


Fig. 4-1 Tensile test of MD CFRP by INSTRON 5982

This experiment is implemented at two times in each case. As increasing the deformation, each fiber is broken and sounds plosive. The fracture is occurred along the fiber orientation. It is because resin has lower strength than the fiber.

As a result of tensile test, MD CFRP with the fiber orientation of 40° , 60° is easily deformed compared to the other with the fiber orientation of 20° . We can conclude shear stress can affect this fracture and shear stress is most critical in the orientation of 45° . Therefore, MD CFRP with the fiber orientation of 40° , 60° is weak with deformation. This result is shown in **Fig. 4-2** and **Fig. 4-3**.

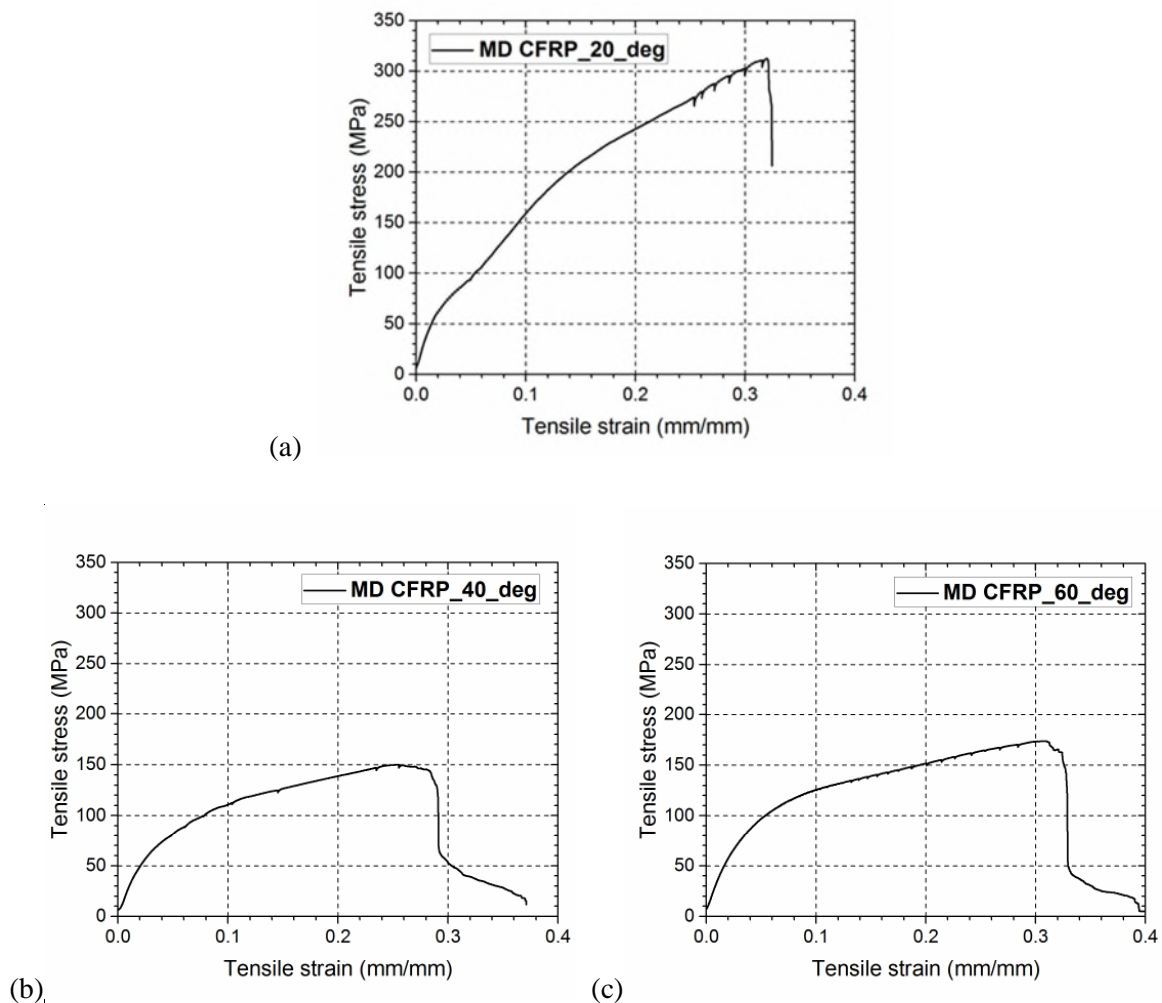


Fig. 4-2 Stress-strain curve of MD CFRP tensile test; (a) 20° , (b) 40° , (c) 60°

In **Fig. 4-2**, there are some fluctuations in tensile strength. It means, each fiber is cut off and stress decreases temporarily. Peak value in these graphs is tensile strength in each fiber orientation. And in **Fig. 4-3**, tensile strength of the cases along the fiber orientation are arranged in one graph.

From tensile strength, we can get shear strength of each fiber orientation by using coordinate transformation. The shear strength can be seen in **Table 4-1**.

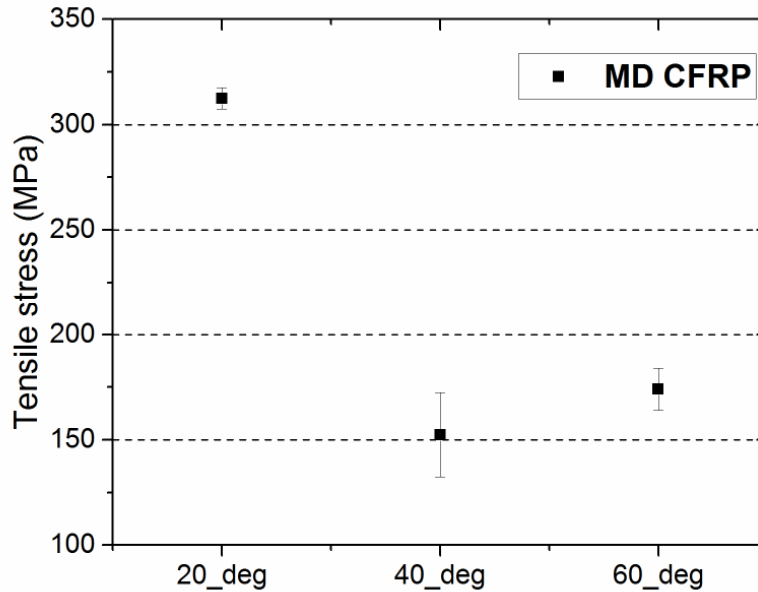


Fig. 4-3 Tensile strength of each fiber orientation in tensile test

Table 4-1 Tensile strength and shear strength of each fiber orientation

Experiment	20_deg	40_deg	60_deg
Tensile strength(MPa)	313.1616	161.9618	177.52725
Shear strength(MPa)	100.65	79.75	76.87

4.1.1.2. Friction test

30*30*3 (mm) MD CFRP workpiece is prepared for friction test. Friction angle is needed to complete numerical model. In friction test, Universal Mechanical & Tribology tester (UMT) is used to find out the coefficient of friction. The method of this friction test is repetitive scratch test. Tip used in this experiment is hard metal with cemented carbide. And tip angle is 45°. The velocity of the tip is 2mm/s and the distance is 20mm. The number of repetition is 10 times. Induced force is 20N.

Firstly, friction is increased rapidly and becomes steady state. As a result of friction test, MD CFRP has about 0.8 friction coefficient in all the fiber orientations, 20°, 40°, 60° as shown in **Fig. 4-4**. From this, we can obtain friction angle by using this equation, $\beta = \tan^{-1}\mu$. β is friction angle, μ is the coefficient of friction.

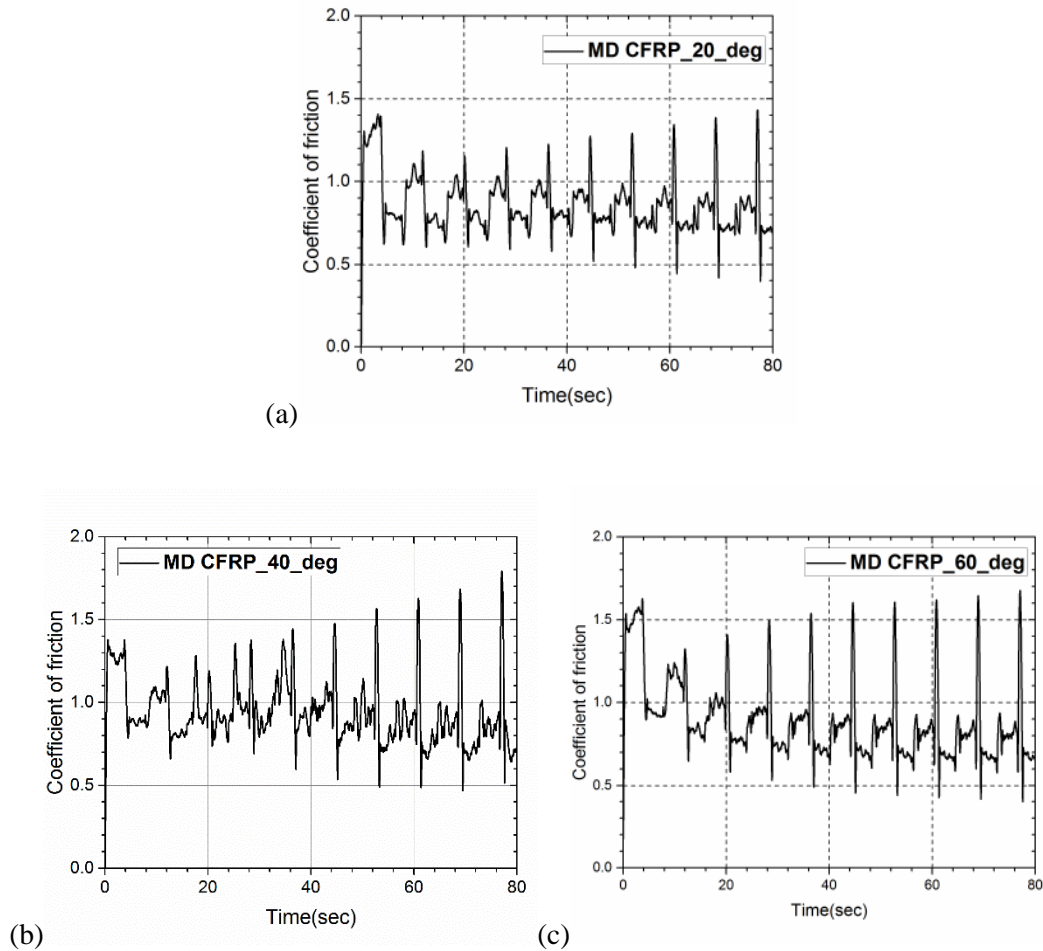


Fig. 4-4 Friction coefficient of each fiber orientation in friction test

4.1.2. Experimental setup

A 3mm multidirectional carbon plain with epoxy resin matrix is used in this experiment as shown in **Fig. 4-5**. This MD CFRP is stacked in 0°/90°. Resin content in this CFRP is 33% and it is thermosetting. The number of prepreg ply is 11. This is made by the method of autoclave which is used to implement industrial processes for elevated temperature and pressure. In this material property, shear strength is obtained by tensile test and fiber's friction angle is from the coefficient

of friction in friction test. Fiber's friction angle is about 38.66° . Epoxy friction coefficient is from 0.4 to 0.5 [41]. So, epoxy friction angle is about 21.8° .

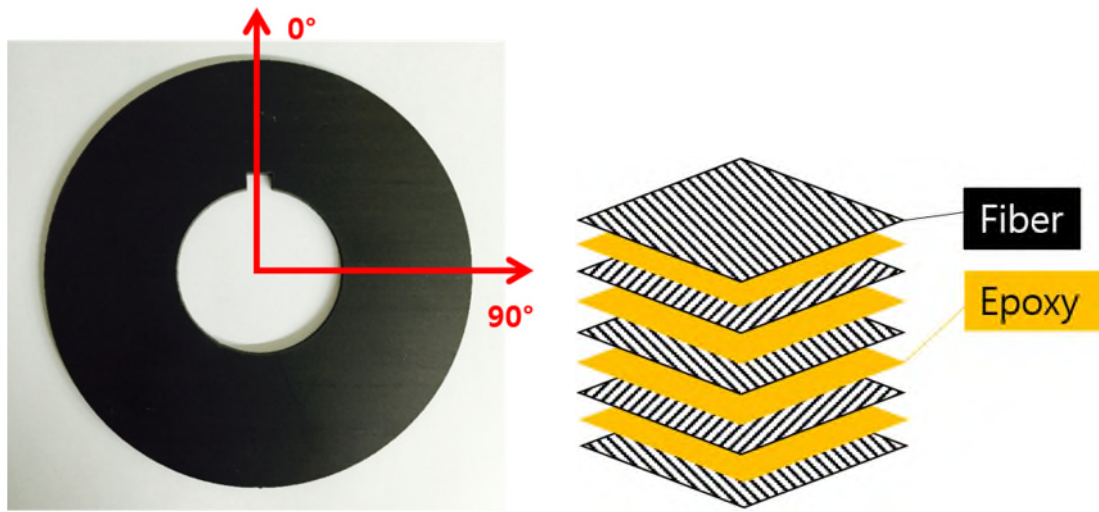


Fig. 4-5 Workpiece of MD CFRP orthogonal cutting

In CFRP orthogonal cutting, insert tool which is uncoated CBN hard metal N123J2-0620-0002-BG H10F from Sandvik corporation. And jig and key are made by SUS material designed as shown in **Fig. 4-6**.

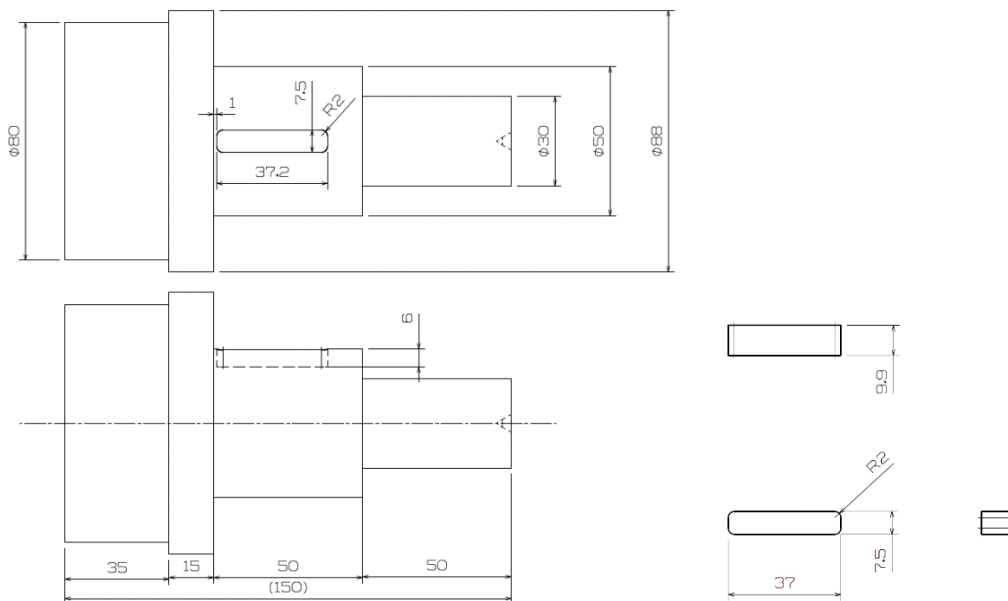


Fig. 4-6 Drawings of jig and key for CFRP orthogonal cutting

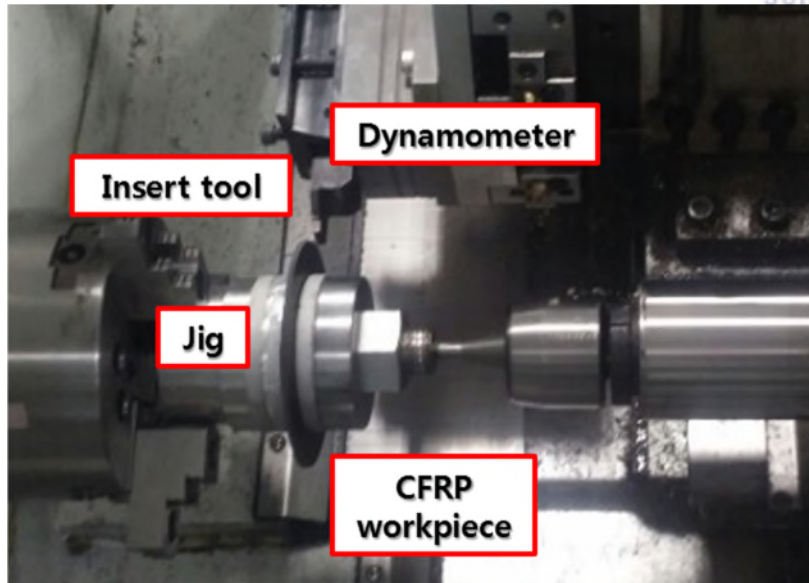


Fig. 4-7 Experimental setup of the orthogonal machining for CFRP material

CNC machine for CFRP orthogonal cutting is decided as TSL-6 model of S&T corporation. Chuck in CNC can fix the jig. And tool dynamometer is chosen as 9127B of KISTLER corporation. Tool is put on this dynamometer. This experimental set can be seen as **Fig. 4-7**.

4.1.3. Comparison between experimental and analytical results

For validate preliminary force prediction model, we compare analytical results with experimental results. The condition of rake angle, γ is 0° . And cutting speed is constant, 80m/min. This comparison can be seen as **Fig. 4-8** in the condition of feed rate 0.15mm/rev. **Fig. 4-8 (a)** is cutting force in each fiber orientation. This cutting force is changed along the fiber orientation because deformation mechanism changes in each condition. Cutting force errors in Bhatnagar's model are 0%, 10.8%, 0% in fiber angle, 20° , 40° , 60° respectively. Cutting force errors in epoxy added preliminary model are 0%, 6.1%, 0% in fiber angle, 20° , 40° , 60° respectively. **Fig. 4-8 (b)** is thrust force in each fiber orientation. Thrust force also changed along the fiber angle. Thrust force errors in Bhatnagar's model are 0%, 0%, 12.4% in fiber angle, 20° , 40° , 60° respectively. Thrust force errors in epoxy added preliminary model are 13.3%, 10%, 9.8% in fiber angle, 20° , 40° , 60° respectively.

The other comparison in the condition of feed rate 0.21mm/rev can be seen as **Fig. 4-9**. Feed rate is faster than previous case. **Fig. 4-9 (a)** is cutting force in each fiber orientation. This cutting force is diverse along the fiber orientation in each condition. Cutting force errors in epoxy added

preliminary model are 5.3%, 0%, 0% in fiber orientation angle, 20°, 40°, 60° respectively. Cutting force errors in epoxy added preliminary model are 5.3%, 0%, 0% in fiber angle, 20°, 40°, 60° respectively. **Fig. 4-9 (b)** is thrust force in each fiber orientation. Thrust force also changed along the fiber orientation angle. Thrust force errors in Bhatnagar’s model are 13.9%, 0%, 10.3% in fiber angle, 20°, 40°, 60° respectively. Thrust force errors in epoxy added preliminary model are 11%, 5.5%, 1% in fiber angle, 20°, 40°, 60° respectively.

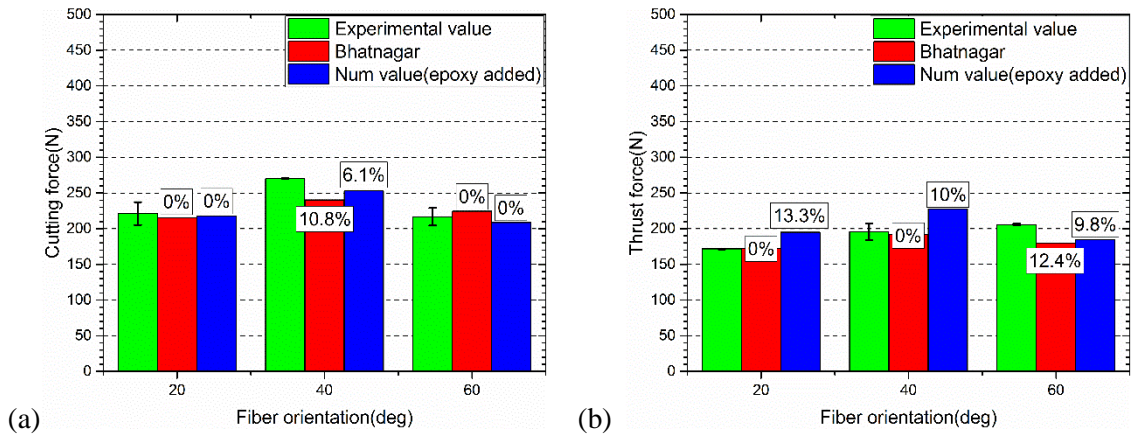


Fig. 4-8 Comparison between numerical and experimental results in terms of (a) cutting forces and (b) thrust forces with cutting speed, 80m/min and feed rate, 0.15mm/rev

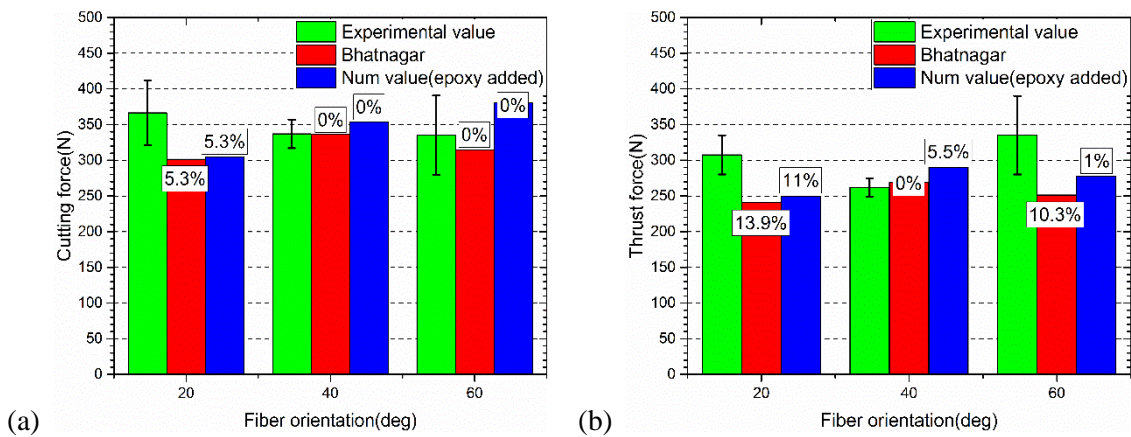


Fig. 4-9 Comparison between numerical and experimental results in terms of (a) cutting forces and (b) thrust forces with cutting speed, 80m/min and feed rate, 0.21mm/rev

Overall, it can be seen that cutting force and thrust force are increased as increasing feed rate in both of the predicted and experimental results. Feed rate can affect the depth of cut and increase area

of machining. In smaller area, Bhatnagar's model has less error than epoxy added preliminary model. On the other hand, preliminary model is more accuracy than Bhatnagar's model in wider area in the condition of feed rate 0.21mm/rev. The reason of this tendency is that epoxy contained in model rises in wider area.

4.1.4. Summary

This preliminary force prediction model can contribute to predict cutting forces in terms of the fiber orientation over 90° defined by the original fiber angle definition. It can help predict damage zone in CFRP machining. Especially, it can enhance the accuracy in high depth of cut. However, this model has limit that it is impossible to establish definite shear strength along each fiber orientation. It is inevitable to select several fiber orientation angles for this model. It is not continuous. For understanding definite cutting mechanism flow of force change, force prediction model according to varying fiber orientation is essential. So, next model from Zhang's model [8] is chosen to develop continuous force prediction model along all the fiber orientation angles.

4.2. Experimental validation of numerical model for predicting force and damage according to varying fiber orientation

It is considered that fiber angle direction is following the original definition of fiber orientation, θ as previously mentioned in **Fig. 3-3**. In this section, modified force prediction model can detect cutting forces change along all the fiber orientations, $0^\circ \leq \theta < 180^\circ$ and we need to compare the numerical model with experimental results for enhancing credibility of prediction. This model was first represented by Zhang [8] and expanded.

4.2.1. Experimental setup

A 3mm unidirectional carbon plain with epoxy resin matrix is used in this experiment as shown in **Fig. 4-10**. Resin content in this UD CFRP is 33% and it is thermoset material. The number of prepreg ply is 11. This is made by the method of autoclave which is used to implement industrial processes for high temperature and high pressure.

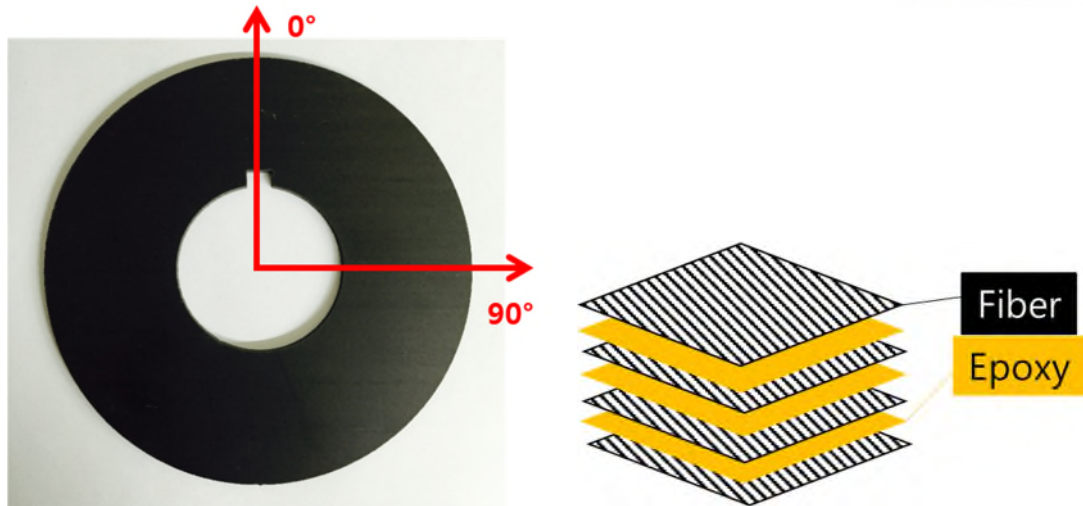


Fig. 4-10 Workpiece of UD CFRP orthogonal cutting

Overall UD CFRP composite material's properties list can be shown in **Table 4-2**. Other experimental equipment setting and method are same as section 4.1. Experimental validation of preliminary model for predicting force. The effective modulus of UD CFRP material in Region 3, E_3 is 4GPa. The workpiece thickness, h is 3mm.

Table 4-2 List of overall UD CFRP composite material's properties

Young's modulus, E	7.7GPa	Shear strength along the fiber, τ_1	85Mpa
Poisson's ratio, ν	0.32	Shear strength normal to the fiber, τ_2	60MPa
Friction angle	30°	Friction coefficient	0.15

4.2.2. Comparison between experimental and analytical results

For identifying certainty of this modified force prediction model, we need to compare analytical results with experimental results. The condition of rake angle, γ is 0°. And clearance angle, α is 7°. In this section, it is assumed that high speed cutting has different mechanism compared to low speed cutting. For this, we decide that first condition is the cutting speed 80m/min and the other condition is the cutting speed 6m/min. Feed rate is constant, 0.15mm/rev.

Overall, we can identify the high fluctuation of force change compared to general metal cutting. It can critically affect the machinability of CFRP cutting. In **Fig. 4-11 (a)**, thrust force is more than cutting force in all range of the fiber orientation in high speed cutting. On the other hand, as shown in **Fig. 4-11 (b)**, thrust force is more than cutting force at first. But cutting force is over the thrust force in fiber orientation over 90° in low speed cutting. Fiber bending in the range of fiber orientation over 90° is occurred more critically in low speed machining condition. It is because chip must be cut before following tool's rake face in high speed cutting and chip can be following tool's rake face in low speed cutting. This bending chip can make the cutting force higher in low speed condition, 6m/min. Cutting force fluctuation is also more critical in low speed cutting. It is the reason of poor machinability in low speed machining condition especially in the range of fiber orientation over 90°.

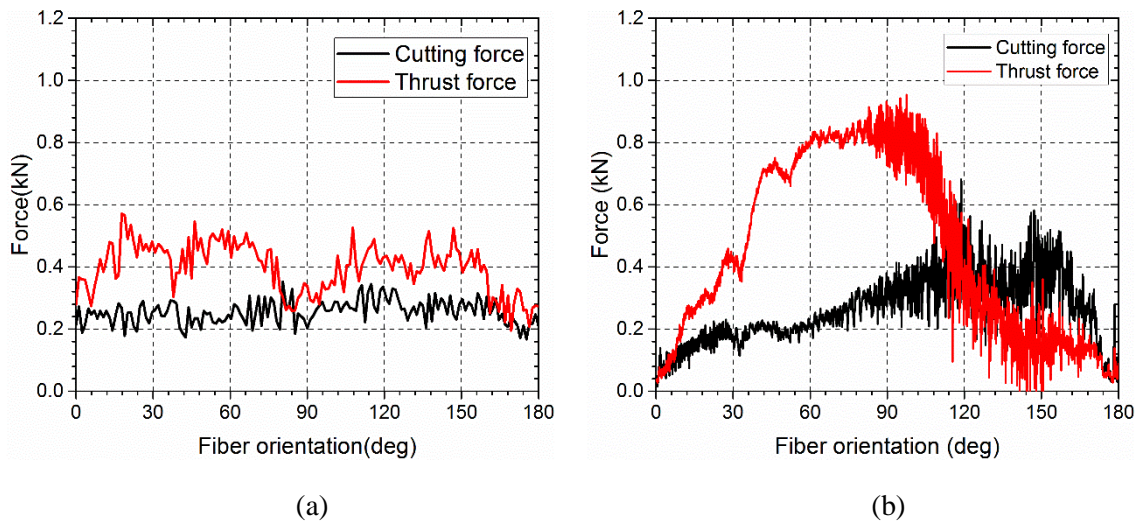


Fig. 4-11 Cutting forces in UD CFRP orthogonal cutting with cutting speed, (a) 80m/min, (b) 6m/min and feed rate, 0.15mm/rev

It can be also verified by chip morphology as shown in **Fig. 4-12** by Scanning Electron Microscope (SEM). In the range of fiber orientation below 90°, fiber can be cut smoothly. On the contrary, in case of fiber orientation over 90°, fiber bending and crush are occurred. Especially, in low speed cutting as shown in **Fig. 4-12 (c)** and **(d)**, the difference along the fiber orientation is remarkable. We can infer fiber bending in the range of fiber orientation over 90° is occurred more critically in low speed machining condition. This result can support that cutting force is over the thrust force in fiber orientation over 90° in low speed cutting. In this study, we concentrate on high speed machining process.

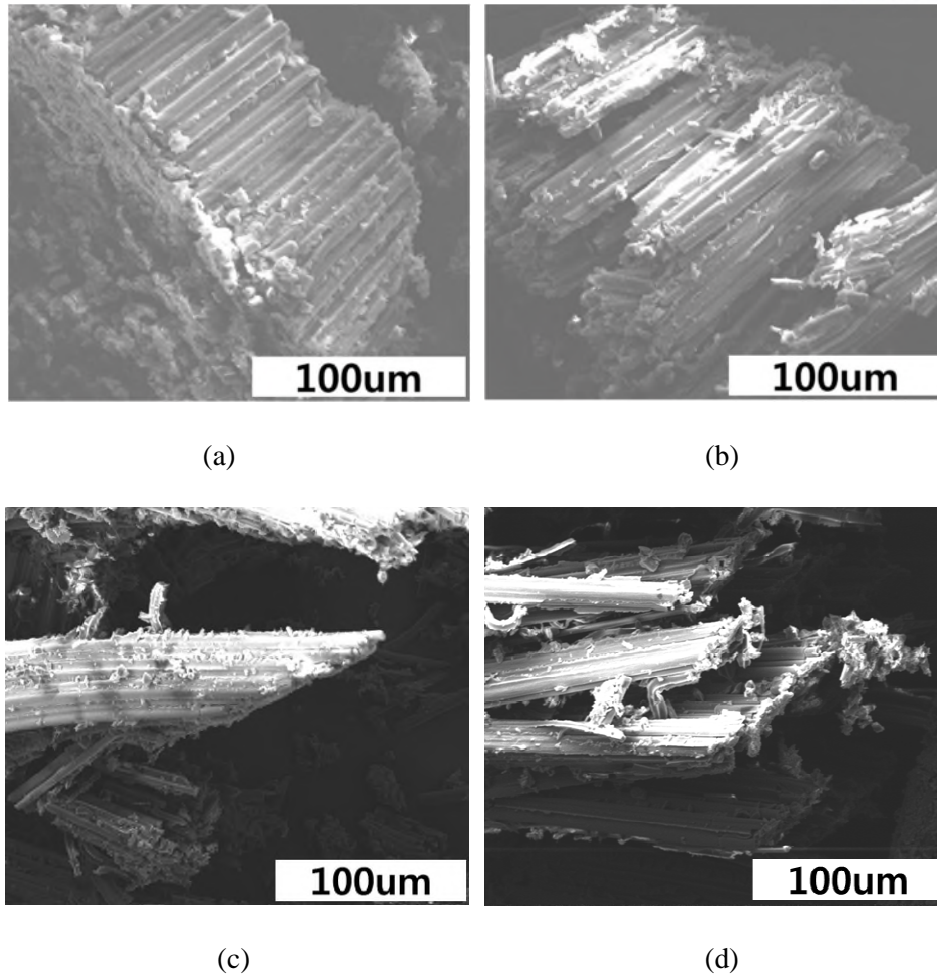


Fig. 4-12 Microscopic image: chip formation in UD CFRP machining with cutting speed 80m/min in (a) $\theta < 90^\circ$, (b) $90^\circ \leq \theta$ and 6m/min in (c) $\theta < 90^\circ$, (d) $90^\circ \leq \theta$

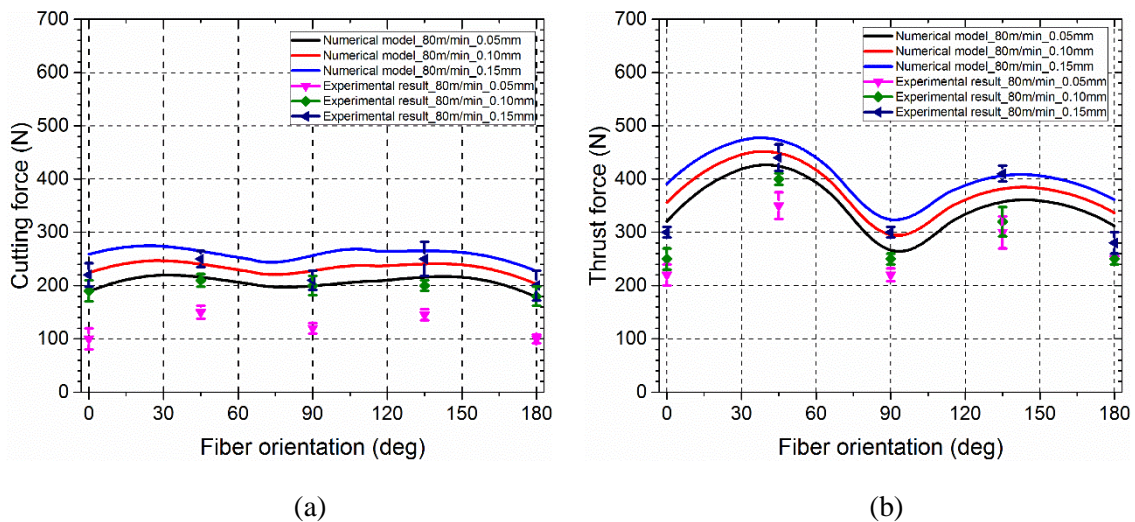


Fig. 4-13 Comparison between numerical and experimental results in terms of (a) cutting forces and (b) thrust forces with cutting speed, 80m/min and feed rate, 0.05, 0.10, 0.15mm/rev

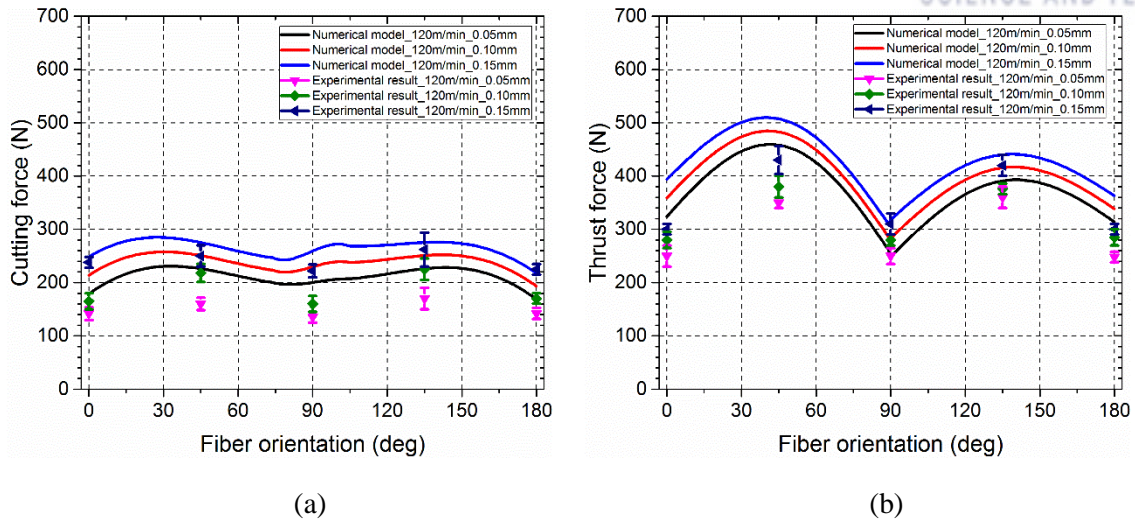


Fig. 4-14 Comparison between numerical and experimental results in terms of (a) cutting forces and (b) thrust forces with cutting speed, 120m/min and feed rate, 0.05, 0.10, 0.15mm/rev

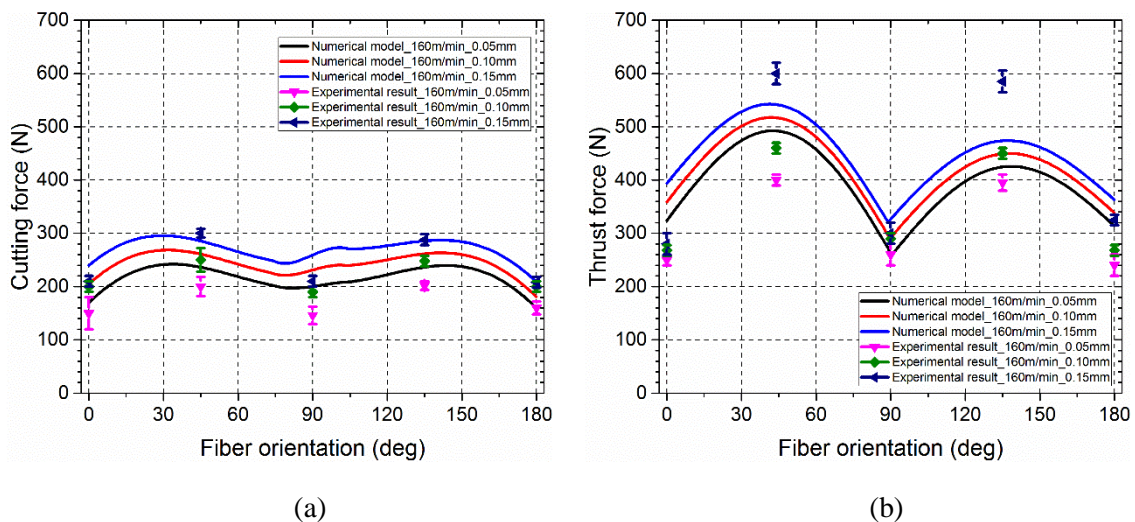


Fig. 4-15 Comparison between numerical and experimental results in terms of (a) cutting forces and (b) thrust forces with cutting speed, 160m/min and feed rate, 0.05, 0.10, 0.15mm/rev

Table 4-3 Cutting forces prediction error with cutting speed, 80m/min

Feed rate(mm/rev)	0.05	0.10	0.15
Cutting force error	Min 9.5% Max 25%	Min 10% Max 27.3%	Min 9.5% Max 25%
Thrust force error	Min 25% Max 50%	Min 15% Max 22.2%	Min 7.7% Max 13.3%

Table 4-4 Cutting forces prediction error with cutting speed, 120m/min

Feed rate(mm/rev)	0.05	0.10	0.15
Cutting force error	Min 2.5% Max 44.4%	Min 1.5% Max 13.6%	Min 2.7% Max 12%
Thrust force error	Min 3% Max 34.3%	Min 5.5% Max 26.3%	Min 3.7% Max 16.7%

Table 4-5 Cutting forces prediction error with cutting speed, 160m/min

Feed rate(mm/rev)	0.05	0.10	0.15
Cutting force error	Min 7.7% Max 12%	Min 5% Max 8 %	Min 2.5% Max 5%
Thrust force error	Min 3.2% Max 27.3%	Min 5.5% Max 10.9%	Min 10% Max 17%

From cutting forces and chip formation analysis, cutting mechanism of the fiber orientation below 90° and over 90° is similar. Therefore, we apply coordinate transfer into numerical solution. On the basis of this numerical solution, continuous cutting force graph can be set and compared to experimental results. As shown in **Fig. 4-13**, **Fig. 4-14** and **Fig. 4-15**, it is suggested that cutting forces tendency of numerical solution is compared to experimental results with cutting speed, 80, 120 and 160m/min. **Table 4-3**, **Table 4-4** and **Table 4-5** suggest error percentage of numerical solution in each condition. As feed rate and cutting speed are increasing, both cutting force and thrust force are increasing. Similar tendency can be seen between numerical solution and experimental results.

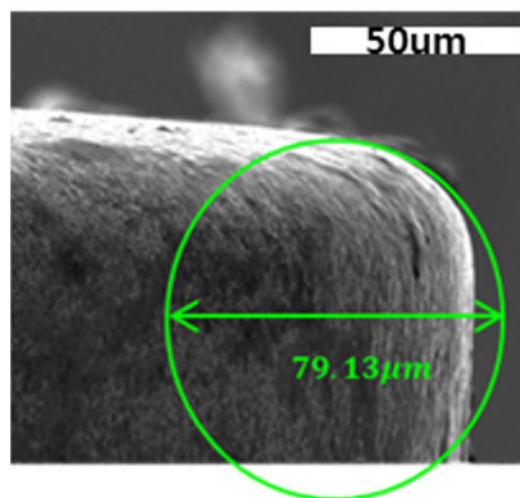


Fig. 4-16 Microscopic image: tool round-edge by scanning electron microscope (SEM)

However, experimental results have lower cutting forces than numerical prediction model in almost all cutting conditions except to the condition of cutting speed, 160m/min and feed rate, 0.15mm/rev. In the condition of low feed rate, cutting depth of cut can be smaller than tool round edge. As shown in **Fig. 4-16**, diameter of tool round edge is 79.13 μ m by Scanning Electron Microscope (SEM). Therefore, pressing force in Region 2 can be decreasing in experiments compared to the numerical solution in low feed rate.

Overall, it can be seen that cutting force and thrust force are increased as increasing feed rate and cutting speed in both of the predicted and experimental results. Feed rate can affect the depth of cut and increase cutting area. Cutting speed can increase amount of tool pressing force. This numerical force prediction model is got from 3 regions of cutting mechanism. This model has tendency of higher cutting forces than experimental results in almost all conditions except to the condition of cutting speed, 160m/min and feed rate, 0.15mm/rev. The reason of this tendency is because round edge of the tool. In conclusion, this modified force prediction model has accuracy from 50% to 98.5%.

4.2.3. Summary

We implement UD CFRP orthogonal cutting for identifying cutting forces change depending on the fiber orientation. In conclusion, we can identify the high fluctuation of force change compared to general metal cutting. It can critically affect the machinability of CFRP cutting.

In addition, suggested force prediction numerical model in this section can contribute to predict cutting forces along all the fiber orientations from 0° to 180° defined by the original fiber angle definition. This model is expanded from Zhang's force prediction model in CFRP machining [8] and cutting mechanism by chip formation. This prediction model has similar tendency of experimental results. Cutting force prediction model accuracy is from 50% to 98.5%. Especially, it can be seen as high accuracy in high feed rate. It is because tool pressing force is decreasing in low feed rate. The error can be generated by other factors in manufacturing UD CFRP workpiece.

Fully developed force prediction model can be used for damage prediction model. It can help predict damage zone along all the fiber orientations in each cutting conditions. Overall, this is objective to develop modified force prediction model according to varying fiber orientation and apply into damage prediction model. This will be optimizing CFRP machining.

4.3. Experimental validation of damage prediction model

The objective of this section is to predict damage zone along all the fiber orientations in each machining condition. And stabilize the prediction by experimental validation in this section. In this section, it is also considered that fiber angle direction is following the original definition of fiber orientation, θ as previously mentioned in **Fig. 3-3**. Previously, force prediction model according to varying fiber orientation is already developed. Based on this solution, we apply into damage prediction model. It was firstly suggested by Jahromi [28]. Work by the cutting force, fiber bending strain energy and matrix shear strain energy are equilibrium by energy balance theory.

4.3.1. Experimental setup

A 3mm unidirectional carbon plain with epoxy thermoset resin matrix is used in this experiment as shown in **Fig. 4-10**. Overall UD CFRP composite material's properties list can be shown in **Table 4-2**. All the experimental equipment setting and method are same as section 4.2. Experimental validation of numerical model for predicting force according to varying fiber orientation.

Additionally, micro-scale material properties are needed in this section. Fiber and epoxy properties list can be shown in **Table 4-6** respectively. This micro-scale properties are referred by Jahromi [28] and T-300 CFRP composite properties.

Table 4-6 List of fiber and epoxy material's properties in UD CFRP composite

Fiber diameter, d_f	7 μ m	Matrix fracture strain, ϵ_m	0.10
Fiber young's modulus, E_f	230Gpa	Matrix shear strength, S_m	146MPa
Fiber flexural strength, X_f	1.8Gpa	Matrix shear modulus, G_m	1.37GPa

4.3.2. Comparison between experimental and analytical results

For identifying accuracy of CFRP damage prediction model, we need to compare numerical solution with experimental results. The condition of rake angle, γ is 0° . And clearance angle, α is 7° . Cutting speed is 80m/min and feed rate is 0.05, 0.10, 0.15mm/rev. After UD CFRP cutting experiments, we observe workpiece internal surface for identifying machinability and defects such as delamination by CT X-ray image as shown in **Fig. 4-17**. We define the average damage length

along the depth including all the layers is final delamination value because it is affected by cutting energy.

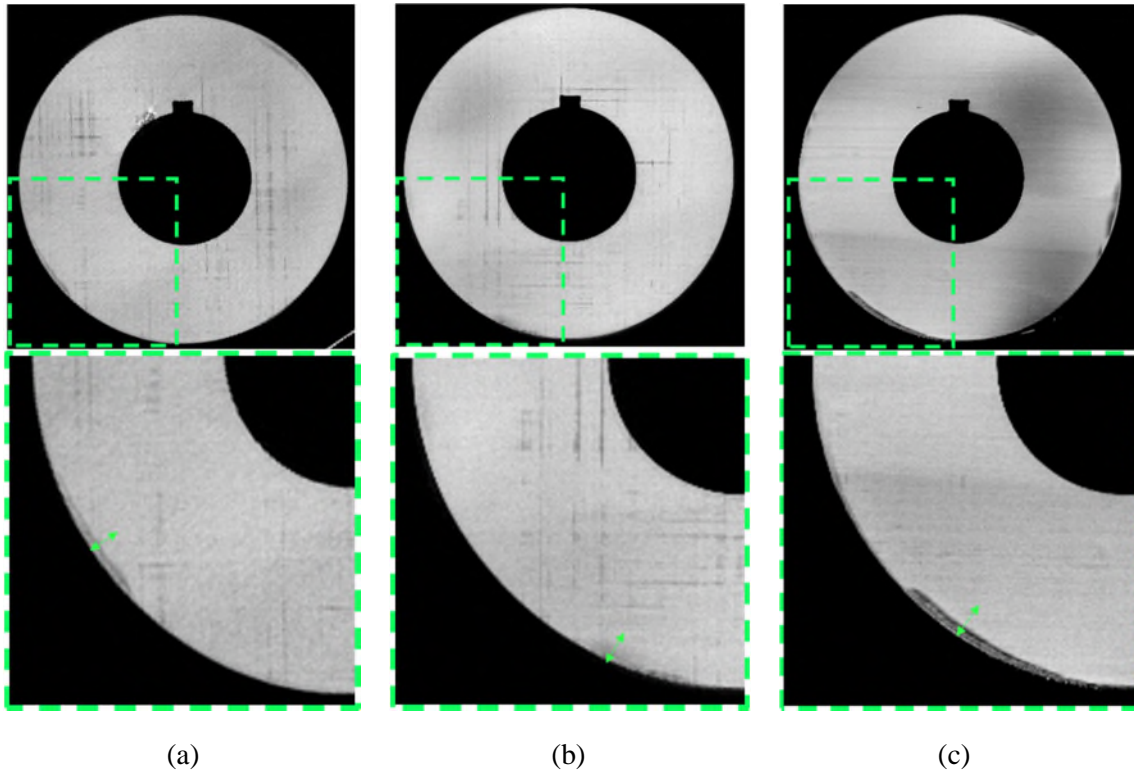


Fig. 4-17 CT X-ray image: internal delamination of UD CFRP machining with cutting speed, 80m/min and feed rate, (a) 0.05, (b) 0.10, (c) 0.15mm/rev

This damage prediction model can contribute to predict defects such as delamination in terms of the fiber orientation defined by the original fiber angle definition. As shown in **Fig. 4-18**, the graph from numerical solution shows similar tendency with experimental results. As we predicted, it shows good machinability along the fiber orientation from 0° to 90° . In the range of fiber orientation from 90° to 180° , it starts making defects inside UD CFRP workpiece. Damage zone is wider in numerical prediction model than experimental results. This result is because damage is occurred in concentration from adhesion of workpiece in experimental case.

High prediction credibility of this damage prediction model can be seen in the condition of fiber orientation from 130° to 150° . There are damage length prediction errors, minimum 2.3%, 12.5% and 1.8% in the condition of feed rate, 0.05, 0.10 and 0.15mm/rev respectively in **Table 4-7**. The errors are from many factors when manufacturing composite materials. Cutting mechanism including fiber strain, matrix strain and fiber matrix decomposition is not simple in experimental execution.

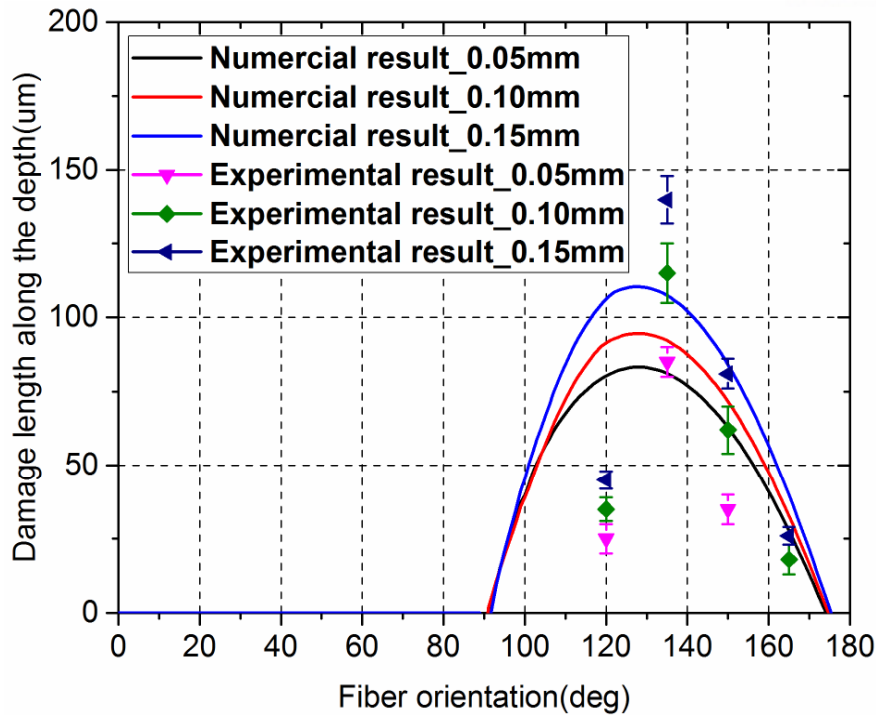


Fig. 4-18 Comparison between numerical and experimental results in terms of damage length with cutting speed, 80m/min and feed rate, 0.05, 0.10, 0.15mm/rev

Table 4-7 Error percentage of damage length prediction model with cutting speed, 80m/min

Feed rate(mm/rev)	0.05	0.10	0.15
Damage length prediction error	Min 2.3%	Min 12.5%	Min 1.8%

4.3.3. Summary

This damage prediction model can contribute to predict defects such as delamination along all the fiber orientation from 0° to 180° defined by the original fiber angle definition. This is contributed by force prediction model according to varying fiber orientation. This prediction model is expanded from Jahromi's force prediction model in CFRP machining [28]. This modified damage prediction model has similar curve tendency as experimental results by CT X-ray. It shows good machinability along the fiber orientation from 0° to 90° . In the range of fiber orientation from 90° to 180° , it starts making defects inside UD CFRP workpiece. Therefore, we need to consider poor machinability in the range of fiber orientation over 90° .

Damage prediction model can help predict amount of damage zone along all the fiber orientations in each cutting conditions. In conclusion, this model is objective to predict and prevent defects such as delamination. This will be optimizing CFRP machining.

5. Conclusions

5.1. Summary

In this study, we try to develop numerical solutions to predict cutting forces and damage along the fiber orientation in each machining condition in CFRP orthogonal cutting. These models are objective to predict and prevent defects such as delamination. This can be optimizing CFRP machining.

Section 2 suggested to analyze the main factors such as fiber orientation, chip formation and delamination affecting CFRP machining. We decided to theoretical model for predicting force and damage in CFRP machining. It is suggested from chip formation and cutting mechanism. This can contain the machining factors in model.

In section 3, we develop numerical models for predicting cutting forces and defects such as delamination along the fiber orientation. There are preliminary force prediction model and force prediction model according to varying fiber orientation. The first one is from Bhatnagar's CFRP force model [7]. This model depends on each separate fiber orientation. The other one is force prediction model according to varying fiber orientation. This model was expanded from Zhang's CFRP force model [8]. From this force prediction model, damage prediction model can be suggested referred to Jahromi's damage prediction model [28]. It is based on energy balance in each fiber material.

In section 4, numerical prediction models are validated by experiments. Firstly, preliminary force prediction model can be seen that cutting force and thrust force are increased as increasing feed rate similar to the experimental results. High feed rate can increase the depth of cut in machining. In smaller area, Bhatnagar's model has less error than epoxy added preliminary model. This developed model is more accuracy than Bhatnagar's model in wider area in the condition of feed rate 0.21mm/rev. The reason is that epoxy region contained in preliminary force prediction model rises in wider area.

Force prediction model according to varying fiber orientation is expanded from Zhang's CFRP force model [8]. Zhang commented this cutting mechanism can be applied only in fiber orientation below 90°. He proved this in low speed CFRP cutting experiments. We did CFRP orthogonal cutting in high cutting speed over 80m/min. We apply similar cutting mechanism into modified model along all the fiber orientation from 0° to 180°. Force prediction model according to varying fiber orientation has similar tendency as the experimental results. The prediction credibility is from 50% to 98.5%. Errors can be generated by many factors in CFRP machining.

From this force prediction model, damage prediction model can be suggested referred to Jahromi's damage prediction model [28]. It is based on energy balance in each fiber material. This damage prediction model has similar curve tendency as experimental results. It shows no defect along the fiber orientation from 0° to 90° . However, in the range of fiber orientation from 90° to 180° , it starts making defects inside UD CFRP workpiece. In conclusion, we need to consider poor machinability in the range of fiber orientation over 90° .

5.2. Conclusions and contributions

This study has objectivity of predicting cutting characteristic such as cutting forces and delamination in CFRP machining. This is validated by experimental results. We apply it into optimizing CFRP machining process and cutting conditions. The main contribution of this project is to establish numerical force prediction model along all the fiber orientations from 0° to 180° in high speed cutting in CFRP machining. Damage prediction model can be also suggested by applying force prediction model according to varying fiber orientation including machining parameters. Lastly, we identify CFRP machining characteristics such as chip formation and delamination by using SEM and CT X-ray equipment.

The principal contributions are:

- (1) Preliminary force prediction model has high accuracy compared to the original model in high feed rate because of epoxy region included but limit as non-continuous force prediction model over 90° in CFRP machining.
- (2) We identify relation of cutting forces vibration and machinability in CFRP machining.
- (3) We identify the difference between high speed cutting and low speed cutting of CFRP orthogonal machining is suggested.
- (4) We discuss about chip formation depending on the fiber orientation and feed rate. It is from chip morphology by using SEM equipment.
- (5) Force prediction model from Zhang can be applied in high speed cutting of CFRP machining and it describes the cutting forces along all the fiber orientation.
- (6) We observe internal defects such as delamination along the fiber orientation by using CT X-ray. Defects are occurred intensively in the range of fiber orientation over 90° in high feed rate.

- (7) From this modified force prediction model, damage prediction model can be suggested based on the energy balance with cutting forces. It includes machining parameters such as feed rate.
- (8) Cutting forces and delamination prediction models of CFRP orthogonal machining can be used to expand the analytical model of CFRP milling and drilling process by coordinate transfer.

5.3. Future work

In this research, numerical models for predicting cutting forces and delamination in CFRP machining are suggested. They are validated by CFRP orthogonal cutting. It is kind of 2 dimensional analysis. Furthermore, we can consider 3 dimensional analysis about CFRP machining. It contains thrust force and delamination of decomposing layers. This model can be referred by Meng's model [42]. Meng's model contains coordinate transfer from 2 dimensional cutting to 3 dimensional cutting. And experimental constant is adjusted. It can be validated by CFRP drilling process. Luo also identifies 3 dimensional drilling model for predicting force and delamination of CFRP and CFRP/Ti stack materials [43, 44].

6. Acknowledgement

First of all, I sincerely appreciate my advisor, Professor. Hyung Wook Park. I have never doubted that his supports and guidance are the most conducive to my research. I also respect his academic knowledge and earnest attitude toward research. I have been motivated and advised many things from him in the process of this work. As one of his disciples, I was able to have much confidence in the mechanical engineering field. I would like to give sincere appreciation to him again.

I am also grateful to my committee members, Professor. Young Bin Park and Professor. Nam Hun Kim. Without their advice and suggestion, this research could not have been complemented by beneficial ideas. Their favor will not be forgotten.

I would like to thank my lab members in Multi-scale Hybrid Manufacturing (MHM) laboratory; Dr. Deka, Dr. Ankita, Dr. Nilanjan, Dr. Eunju Park, Dr. Kyoungil Kong, Dr. Dongmin Kim, Jisu Kim, Jaewoo Seo, Ineon Lee, Doyoung Kim, Minji Kim, Wujin Lee and Yeonoh Kim for their supports. And it was very fortunate for me to be with them.

Presently, I'd like to mention my gratitude toward my family for their supports and trust. Without both my father and mother's dedication so far, I could not have been who I am today. In particular, my sister has always encouraged me to be confident in my work well.

Lastly, I cordially express my special thanks to the other people who have been with me but not mentioned here.

I dedicate this thesis to my advisor, committee members, lab members and acquaintances for their constant support and unconditional helps. I love you all dearly.

Reference

1. Arul, S., et al., *Influence of tool material on dynamics of drilling of GFRP composites*. The International Journal of Advanced Manufacturing Technology, 2006. **29**(7-8): p. 655-662.
2. Mallick, P.K., *Composites engineering handbook*. 1997: CRC Press.
3. Schwartz, M.M., *Composite materials handbook*. 1984: McGraw-Hill.
4. Mallick, P.K., *Fiber-reinforced composites: materials, manufacturing, and design*. 2007: CRC press.
5. Mk, N.K., et al., *Tool wear and surface roughness on milling carbon fiber-reinforced plastic using chilled air*. Journal of Asian Scientific Research, 2012. **2**(11): p. 593.
6. Grilo, T.J., et al., *Experimental delamination analyses of CFRPs using different drill geometries*. Composites Part B: Engineering, 2013. **45**(1): p. 1344-1350.
7. Bhatnagar, N., et al., *On the machining of fiber reinforced plastic (FRP) composite laminates*. International Journal of Machine Tools and Manufacture, 1995. **35**(5): p. 701-716.
8. Zhang, L.C., H.J. Zhang, and X.M. Wang, *A Force Prediction Model for Cutting Unidirectional Fibre-Reinforced Plastics*. Machining Science and Technology, 2001. **5**(3): p. 293-305.
9. Hollaway, L., *Key issues in the use of fibre reinforced polymer (FRP) composites in the*

- rehabilitation and retrofitting of concrete structures*. Service life estimation and extension of civil engineering structures, 2011: p. 8.
10. Rajasekaran, T., K. Palanikumar, and B. Vinayagam, *Turning CFRP composites with ceramic tool for surface roughness analysis*. Procedia Engineering, 2012. **38**: p. 2922-2929.
 11. Fujiwara, J., T. Kawazoe, and N. Matsui. *Cutting Mechanism of Sulfrized Free-Machining Steel*. in *Key Engineering Materials*. 2009. Trans Tech Publ.
 12. Chennakesavelu, G., *Orthogonal machining of uni-directional carbon fiber reinforced polymer composites*. 2010, Wichita State University.
 13. Sorrentino, L. and S. Turchetta, *Cutting forces in milling of carbon fibre reinforced plastics*. International Journal of Manufacturing Engineering, 2014. **2014**.
 14. Davim, J.P. and P. Reis, *Damage and dimensional precision on milling carbon fiber-reinforced plastics using design experiments*. Journal of materials processing technology, 2005. **160**(2): p. 160-167.
 15. Liu, G., et al., *Surface Quality of Staggered PCD End Mill in Milling of Carbon Fiber Reinforced Plastics*. Applied Sciences, 2017. **7**(2): p. 199.
 16. Chen, W.-C., *Some experimental investigations in the drilling of carbon fiber-reinforced plastic (CFRP) composite laminates*. International Journal of Machine Tools and Manufacture, 1997. **37**(8): p. 1097-1108.
 17. Brinksmeier, E. and R. Janssen, *Drilling of multi-layer composite materials consisting of carbon fiber reinforced plastics (CFRP), titanium and aluminum alloys*. CIRP Annals-

- Manufacturing Technology, 2002. **51**(1): p. 87-90.
18. Sheikh-Ahmad, J. and R. Yadav, *Model for predicting cutting forces in machining CFRP*. International Journal of Materials and Product Technology, 2008. **32**(2-3): p. 152-167.
 19. Eneyew, E.D. and M. Ramulu, *Experimental study of surface quality and damage when drilling unidirectional CFRP composites*. Journal of Materials Research and Technology, 2014. **3**(4): p. 354-362.
 20. Rao, G.V.G., P. Mahajan, and N. Bhatnagar, *Micro-mechanical modeling of machining of FRP composites–Cutting force analysis*. Composites science and technology, 2007. **67**(3): p. 579-593.
 21. Rahman, M., et al., *Machinability study of carbon fiber reinforced composite*. Journal of materials processing technology, 1999. **89**: p. 292-297.
 22. Voß, R., et al., *Chip root analysis after machining carbon fiber reinforced plastics (CFRP) at different fiber orientations*. Procedia CIRP, 2014. **14**: p. 217-222.
 23. Calzada, K.A., et al., *Modeling and interpretation of fiber orientation-based failure mechanisms in machining of carbon fiber-reinforced polymer composites*. Journal of Manufacturing Processes, 2012. **14**(2): p. 141-149.
 24. DeBoer, J., S. Vermilyea, and R. Brady, *The effect of carbon fiber orientation on the fatigue resistance and bending properties of two denture resins*. The Journal of prosthetic dentistry, 1984. **51**(1): p. 119-121.
 25. Wei, Y., et al., *Influence of fiber orientation on single-point cutting fracture behavior of carbon-fiber/epoxy prepreg sheets*. Materials, 2015. **8**(10): p. 6738-6751.

26. Santiuste, C., et al., *Delamination prediction in orthogonal machining of carbon long fiber-reinforced polymer composites*. Journal of Reinforced Plastics and Composites, 2012. **31**(13): p. 875-885.
27. Bhatnagar, N., et al., *Determination of machining-induced damage characteristics of fiber reinforced plastic composite laminates*. Materials and Manufacturing Processes, 2004. **19**(6): p. 1009-1023.
28. Jahromi, A.S., B. Bahr, and K.K. Krishnan, *An analytical method for predicting damage zone in orthogonal machining of unidirectional composites*. Journal of Composite Materials, 2014. **48**(27): p. 3355-3365.
29. Takeyama, H. and N. Iijima, *Machinability of glassfiber reinforced plastics and application of ultrasonic machining*. CIRP Annals-Manufacturing Technology, 1988. **37**(1): p. 93-96.
30. Abena, A., S.L. Soo, and K. Essa, *A finite element simulation for orthogonal cutting of UD-CFRP incorporating a novel fibre-matrix interface model*. Procedia CIRP, 2015. **31**: p. 539-544.
31. Pwu, H. and H. Hocheng, *Chip formation model of cutting fiber-reinforced plastics perpendicular to fiber axis*. Journal of manufacturing science and engineering, 1998. **120**(1): p. 192-196.
32. Lasri, L., M. Nouari, and M. El Mansori, *Modelling of chip separation in machining unidirectional FRP composites by stiffness degradation concept*. Composites Science and Technology, 2009. **69**(5): p. 684-692.

33. Kim, K.S., Y.K. Kwak, and S. Namgung, *Machinability of carbon fiber-epoxy composite materials in turning*. Journal of Materials Processing Technology, 1992. **32**(3): p. 553-570.
34. Everstine, G. and T. Rogers, *A theory of machining of fiber-reinforced materials*. Journal of Composite Materials, 1971. **5**(1): p. 94-106.
35. KoPlev, A., A. Lystrup, and T. Vorm, *The cutting process, chips, and cutting forces in machining CFRP composites*, 1983. **14**(4): p. 371-376.
36. Wang, D., M. Ramulu, and D. Arola, *Orthogonal cutting mechanisms of graphite/epoxy composite. Part I: unidirectional laminate*. International Journal of Machine Tools and Manufacture, 1995. **35**(12): p. 1623-1638.
37. Wang, X. and L. Zhang, *An experimental investigation into the orthogonal cutting of unidirectional fibre reinforced plastics*. International Journal of Machine Tools and Manufacture, 2003. **43**(10): p. 1015-1022.
38. Jahromi, A.S. and B. Bahr, *An analytical method for predicting cutting forces in orthogonal machining of unidirectional composites*. Composites Science and Technology, 2010. **70**(16): p. 2290-2297.
39. Qi, Z., et al., *Microscopic mechanism based force prediction in orthogonal cutting of unidirectional CFRP*. The International Journal of Advanced Manufacturing Technology, 2015. **79**(5-8): p. 1209-1219.
40. Chen, L., et al., *A cutting force predicting model in orthogonal machining of unidirectional CFRP for entire range of fiber orientation*. The International Journal of

- Advanced Manufacturing Technology, 2016: p. 1-14.
41. Alajmi, M. and A. Shalwan, *Correlation between Mechanical Properties with Specific Wear Rate and the Coefficient of Friction of Graphite/Epoxy Composites*. Materials, 2015. **8**(7): p. 4162-4175.
 42. Meng, Q, et al., *An analytical method for predicting the fluctuation of thrust force during drilling of unidirectional carbon fiber reinforced plastics*. Journal of Composite Materials, 2015. **49**(6): p. 699-711.
 43. Luo, B., et al., *A novel prediction model for thrust force and torque in drilling interface region of CFRP/Ti stacks*. The International Journal of Advanced Manufacturing Technology, 2015. **81**(9-12): p. 1497-1508.
 44. Luo, B., et al., *Effect of workpiece stiffness on thrust force and delamination in drilling thin composite laminates*. Journal of Composite Materials, 2016. **50**(5): p. 617-625.